The Journal of Eukaryotic Microbiology

Published by the International Society of Protistologists

Journal of Eukaryotic Microbiology ISSN 1066-5234

ORIGINAL ARTICLE

A New Heterotrophic Dinoflagellate from the North-eastern Pacific, *Protoperidinium fukuyoi*: Cyst–Theca Relationship, Phylogeny, Distribution and Ecology

Kenneth N. Mertens[a], Aika Yamaguchi[b,c], Yoshihito Takano[d], Vera Pospelova[e], Martin J. Head[f], Taoufik Radi[g], Anna J. Pieńkowski[h], Anne de Vernal[g], Hisae Kawami[d] & Kazumi Matsuoka[d]

a Research Unit for Palaeontology, Ghent University, Krijgslaan 281 s8, 9000, Ghent, Belgium
b Okinawa Institution of Science and Technology, 1919-1 Tancha, Onna-son, Kunigami, Okinawa, 904-0412, Japan
c Kobe University Research Center for Inland Seas, Rokkodai, Kobe, 657-8501, Japan
d Institute for East China Sea Research (ECSER), 1-14, Bunkyo-machi, Nagasaki, 852-8521, Japan
e School of Earth and Ocean Sciences, University of Victoria, OEASB A405, P. O. Box 1700 STN CSC, Victoria, British Columbia, V8W 2Y2, Canada
f Department of Earth Sciences, Brock University, 500 Glenridge Avenue, St. Catharines, Ontario, L2S 3A1, Canada
g GEOTOP, Université du Québec à Montréal, P. O. Box 8888, Montréal, Qubec, H3C 3P8, Canada
h School of Ocean Sciences, College of Natural Sciences, Bangor University, Menai Bridge, Anglesey, LL59 5AB, United Kingdom

Keywords
LSU rDNA; round spiny brown cyst; Saanich Inlet; San Pedro Harbor; single-cell PCR; SSU rDNA; Strait of Georgia.

Correspondence
K. Mertens, Research Unit for Palaeontology, Ghent University, Krijgslaan 281 s8, 9000 Ghent, Belgium
Telephone number: +32-9-264-4609;
FAX number: +32-9-264-4608;
e-mail: kenneth.mertens@ugent.be

Received: 31 January 2013; revised 3 April 2013; accepted April 3, 2013.

doi:10.1111/jeu.12058

ABSTRACT

The cyst–theca relationship of *Protoperidinium fukuyoi* n. sp. (Dinoflagellata, Protoperidiniaceae) is established by incubating resting cysts from estuarine sediments off southern Vancouver Island, British Columbia, Canada, and San Pedro Harbor, California, USA. The cysts have a brown-coloured wall, and are characterized by a saphopylic archeopyle comprising three apical plates, the apical pore plate and canal plate; and acuminate processes typically arranged in linear clusters. We elucidate the phylogenetic relationship of *P. fukuyoi* through large and small subunit (LSU and SSU) rDNA sequences, and also report the SSU of the cyst-defined species *Islandinium minutum* (Harland & Reid) Head et al. 2001. Molecular phylogenetic analysis by SSU rDNA shows that both species are closely related to *Protoperidinium americanum* (Gran & Braarud 1935) Balech 1974. Large subunit rDNA phylogeny also supports a close relationship between *P. fukuyoi* and *P. americanum*. Three subgroups in total are further characterized within the *Monovela* group. The cyst of *P. fukuyoi* shows a wide geographical range along the coastal tropical to temperate areas of the North-east Pacific, its distribution reflecting optimal summer sea-surface temperatures of ~14–18 °C and salinities of 22–34 psu.

FREE-LIVING marine dinoflagellates comprise a diverse group of organisms, currently encompassing approximately 1,555 species (Gómez 2005). In addition to a motile stage, some dinoflagellates produce resting cysts as part of their life cycle, allowing them to endure unfavourable environmental conditions. Resting cysts are assumed to be hypnozygotes based on the relatively few species for which this has been confirmed (e.g. Figueroa et al. 2011; von Stosch 1973), and resting cysts are usually the only geologically preservable stage in the dinoflagellate life cycle. The existence of these two life cycle stages has resulted in the creation of two taxonomic systems: one used by biologists and based on the morphology of living motile cells, and the other developed by palaeontologists and based on resting cyst morphology. Linking both stages is important for both biological and geological studies. This was traditionally established by incubating living cysts and identifying the emergent motile stage (e.g. Wall and Dale 1968). Molecular analyses are now an important additional tool, utilizing the polymerase chain reaction (PCR) technique either on single cells or single cysts (e.g. Bolch 2001; Matsuoka and Head in press; Matsuoka et al. 2006; Takano and Horiguchi 2006).

Some cysts are brown in colour with a distinct spheroidal, process-bearing shape and are therefore informally designated as round brown spiny cysts (Radi et al. 2013). Two cyst-defined genera, using palaeontological nomenclature, presently accommodate these species. Cysts

belonging to the genus *Echinidinium* Zonneveld 1997 ex Head et al. 2001 are characterized by a theropylic archeopyle (Head et al. 2001), i.e. an angular slit that follows plate boundaries but without complete release of plates (Matsuoka 1988). Cysts belonging to the genus *Islandinium* Head et al. 2001 open with a saphopylic archeopyle, which is defined as having a free operculum (Matsuoka 1988). At the species level, process (spine), characteristics (hollow or solid, size, lateral profile, surface ornamentation including striations or spinules, heterogeneity, density of distribution) and wall texture (granular to smooth) are important attributes for distinguishing species (e.g. Head 2003; Head et al. 2001; Mertens et al. 2012a; Pospelova and Head 2002; Radi et al. 2013; Zonneveld 1997).

Cyst–motile stage relationships have been established for very few species producing round brown spiny cysts, these being: *Diplopelta parva* (Matsuoka 1988), *Protoperidinium monospinum* (Zonneveld & Dale 1994), *Oblea acanthacysta* (Kawami et al. 2006), *Protoperidinium tricingulatum* (Kawami et al. 2009), and several cyst morphotypes of *Archaeperidinium minutum* (Mertens et al. 2012a; Ribeiro et al. 2010) and the closely related species *Archaeperidinium saanichi* (both reviewed in Mertens et al. 2012a). *Archaeperidinium minutum* was previously called *Protoperidinium minutum*, the genus *Archaeperidinium* having been reinstated by Yamaguchi et al. (2011) based on morphological and phylogenetic observations. No cyst-defined names have been erected for any of these motile-stage defined species, mostly to avoid unnecessary taxonomic complexity. However, with the advent of molecular techniques, it has become increasingly apparent that cyst characteristics such as the archeopyle (e.g. Matsuoka 1988; Matsuoka and Head in press) and thecal characteristics including details of the sulcal plates – as suggested early by Abé (1936) and more recently by Matsuoka and Kawami (in press) – are of primary importance in grouping species.

In addition to their taxonomic interest, these round brown spiny cysts are important for palaeoclimatological studies because their distributions are related to temperature, salinity, trophic state and sea-ice cover (Radi et al. 2013; Zonneveld et al. 2013). Some species, notably *Echinidinium karaense*, *Islandinium minutum* and *Islandinium*? *cezare* s.l., have distinct cold-water distributions (Head et al. 2001) and have been associated with sea-ice cover (e.g. Radi et al. 2013). Recent molecular work reveals the presence of *Islandinium* sp. or its motile stage in Canadian sea-ice for the first time (Comeau et al. 2013). Other species, including *Echinidinium bispiniformum*, have a distinct warm-water distribution (Zonneveld 1997).

Here, we report the germination of a new morphotype of round brown spiny cysts collected from surface sediments underlying estuarine waters off southern Vancouver Island, British Columbia, Canada, and San Pedro Harbor, California, USA, and provide the results of molecular analysis. The cyst has a saphopylic, *Islandinium*-type archeopyle and belongs to a previously undescribed species, *Protoperidinium fukuyoi* n. sp. Molecular phylogenetic analyses inferred by SSU rDNA show that it is closely related to *Protoperidinium americanum*, *Protoperidinium fusiforme*, *Protoperidinium parthenopes, P. tricingulatum* and the cyst-defined species *I. minutum.* By quantitatively documenting the cyst in surface sediments and sediment traps, we show its wide distribution along the northwest American margin.

MATERIALS AND METHODS

Incubation studies were performed by K.N.M. at the Institute for East China Sea Research at Nagasaki University. Molecular work was carried out at the same location by Y.T. and H.K. Palynological work was conducted by V.P., T.R. and M.J.H. at the University of Victoria, GEOTOP, and Brock University, respectively.

Germination experiments

To obtain cysts of *P. fukuyoi* n. sp. for incubation studies, surface sediment samples containing round brown spiny cysts were collected at three locations around southern Vancouver Island, British Columbia, Canada, in October 2011: (1) Patricia Bay, Saanich Inlet (site A), (2) Brentwood Bay, Saanich Inlet (site B), and (3) central Strait of Georgia (site C) and two locations around San Pedro Harbor, California, USA (sites E and F) (Table 1 and Fig. S1). The studied cyst type had been previously identified as "cyst type A" in the following North Pacific settings: the Strait of Georgia (Pospelova et al. 2010; Radi et al. 2007), coastal bays of southern Vancouver Island (Krepakevich and Pospelova 2010), Saanich Inlet (Price and Pospelova 2011), the Santa Barbara Basin (Bringué et al. 2013; Pospelova et al. 2006), and off Mexico (Limoges et al. 2010). All samples were stored in plastic bags in a refrigerator at 4 °C. In situ sea-surface salinities (SSSs) and sea-surface temperatures (SSTs) were measured when collecting samples (Table S1).

About 0.5–1.0 cm^3 of wet sediment was immersed in filtered seawater and, after 1 min of ultrasonication using an As One™ (As One Corp., Osaka, Japan) US2R ultrasonic bath, the sediment was rinsed through a 20 μm metallic-meshed calibrated Sanpo™ (Sanpo, Tokyo, Japan) sieve using filtered seawater. From this residue, the cyst fraction was separated using the heavy-liquid sodium polytungstate at a density of 1.3 g/cm (Bolch 1997). Single cysts were then transferred to Nunclon (Thermo Fisher Scientific, Hannover, Germany) 0.5 ml microwells subjected to an irradiance of 100 μmol photons/m^2/s and 24-h light, and filled with ESM medium (Watanabe et al. 2000) at temperatures and salinities comparable to the respective natural environments (Table S1). Cysts were regularly checked for germination, and observations were performed under an Olympus IX70 (Olympus, Tokyo, Japan) inverted light microscope. Encysted and excysted cysts and motile cells were photographed and measured using an Olympus BX51 (Olympus) light microscope with a Nikon digital sight DS-1L 1 module (Nikon, Tokyo, Japan) with 100X oil immersion objectives. For each motile cell, the length and width were

Table 1. Details of locations for incubation experiments and single-cell PCR analyses

Purpose of sample	Station	Location	Latitude (°N)	Longitude (°E)	Water depth (m)	Sampled by	Sampling device	Sampling date	In situ SST (°C)	In situ SSS (psu)	Ref
INC	A	Patricia Bay, SI, VENUS Station, BC	48.651	−123.487	95	RV	R	2011-10-01	10.0	~30.5	This study
I/P	B	Brentwood Bay, SI, BC	48.577	−123.468	6	AP	PPG	2011-10-01	9.1	32.1	This study
INC	C	Central Strait of Georgia, VENUS Station, BC	49.040	−123.426	300	RV	V	2011-10-02	~14	28.5	This study
INC	D	Oak Bay, BC	48.425	−123.301	9	VP	PPG	2010-10-09	10.4	31.3	(1)
INC	E	San Pedro Harbor St. 1, CA	33.736	−118.270	7	VP	PPG	2011-08-25	20.2	32.2	This study
INC	F	San Pedro Harbor St. 2, CA	33.743	−118.248	5	VP	PPG	2011-08-25	20.2	32.2	(2)
I/P	G	Barrow Strait, Nunavut, Canada	74.246	−91.495	316	AJP	BC	2011-10-12	NA	NA	This study
PCR	NA	Off Nagayo, Japan	32.867	129.871	NA	HK	PN	2004-07-09	NA	NA	This study
PCR	NA	Off Mie, Japan	32.811	129.772	NA	HK	PN	2004-05-05	NA	NA	This study
PCR	NA	Off Sasebo, Japan	33.162	129.724	NA	HK	PN	2008-02-26	NA	NA	This study

1 = Mertens et al. (2012a); 2 = Mertens et al.(2012b).
NA = not acknowledged; INC = incubation; PCR = single-cell PCR; I/P = incubation and single-cyst PCR; SI = Saanich Inlet; BC = British Columbia; CA = California; RV = R/V Thompson, Vera Pospelova; AP = Andrea Price; VP = Vera Pospelova; AJP = Anna Pienkowski; HK = Hisae Kawami; PPG = Petite Ponar Grab; R = Ropos; V = Venus-Ropos; BC = Boxcore; PN = Plankton net.

measured. For each cyst, the longest and shortest body diameter and five processes were measured.

We also tried to germinate *I. minutum* from Barrow Strait, northern Canada but none of the 173 isolated spiny round brown cysts germinated.

Study of cysts from sediment trap samples, surface sediment and downcore

To determine the distribution of the studied cysts, permanent slides of previously studied surface samples and sediment trap samples were reinvestigated, which included locations from coastal BC and the north-eastern Pacific (Table S1 and Fig. S1). Three sediment cores were also investigated for the occurrence of this species: Strait of Georgia (CM3, Pospelova et al. 2010), ODP 893A (Santa Barbara Basin, Pospelova et al. 2006) and MD02-2515 (Guaymas Basin, Price et al. 2013) (Table S1 and Fig. S1). Palynological techniques were used for processing (Pospelova et al. 2004; Price and Pospelova 2011). The samples were oven-dried at 40 °C and then treated with room temperature 10% HCl to remove calcium carbonate particles. Material was rinsed twice with distilled water, sieved at 120 μm to eliminate coarse material and retained on a 15 μm nylon mesh. To dissolve siliceous particles, samples were treated with 48–50% room temperature hydrofluoric acid for 2 d, and then treated for 10 min with room-temperature HCl (10%) to remove fluorosilicates. The residue was rinsed twice with distilled water, ultrasonicated for 30 s and finally collected on a 15 μm mesh. Aliquots of residue were mounted in glycerine jelly.

All measurements and light photomicrographs were obtained by K.N.M., M.J.H and V.P., respectively, using an Olympus BX51 with a Nikon digital sight DS-1L 1 module, a Leica DMR microscope with a Leica DFC490 digital camera (Leica, Solms, Germany), and a Nikon Eclipse 80i transmitting light microscope with a DS-L2 module, all with 100X oil immersion objectives. All cyst and motile cell measurements in the species descriptions cite the minimum, average (in parentheses) and maximum values (μm), in that order. The standard deviation (SD) is also provided where appropriate. For scanning electron microscope (SEM) observations, cysts were isolated from a sample from the CM3 sediment trap (UVic 2008-114) located in the Strait of Georgia (in the proximity of site C on Fig. S1) covering a sampling interval between 2 June 1998 and 14 June 1998 (Pospelova et al. 2010) using a micropipette. Cysts were rinsed several times in distilled water, placed on stubs, dried for 2 wk, sputter coated with gold, and examined using a Hitachi S-3500N (Hitachi, Tokyo, Japan) SEM at the Electron Microscopy Laboratory, Biology Department, University of Victoria.

Single-cell PCR amplification and sequencing of cysts of *Protoperidinium fukuyoi* and *Islandinium minutum*

Surface sediment samples containing cysts of *P. fukuyoi* were collected from Brentwood Bay, Saanich Inlet, British Columbia, Canada (Table 1 and Fig. S1). Surface sediment samples containing the cyst-defined species *I. minutum* were collected from Barrow Strait, Nunavut, Canada (Fig. S1 and Table 1). Cysts were isolated from the sediment using

heavy liquid separation as described above. Isolated cysts were ultrasonicated in a 200 μl PCR tube with sterilized seawater. The cysts were individually transferred to a glass slide covered with a frame of vinyl tape, and photographed using an Olympus BX51 microscope with an Olympus DP71 digital camera. Each cyst was transferred to an inverted light microscope and crushed with a fine glass needle, and subsequently transferred into a 200 μl PCR tube containing 3 μl of Milli-Q water. Sequences of SSU and partial LSU rDNA were determined from single cysts of *P. fukuyoi* but only SSU rDNA sequences for *I. minutum*. In the first round of PCR, the external primers SR1 and LSU R2 (Takano and Horiguchi 2006) were used with PCR mixtures of KOD-Plus-Ver. 2 Kit (Toyobo, Osaka, Japan), and the PCR conditions applied were: one initial cycle of denaturation at 94 °C for 2 min, followed by 35 cycles of denaturation at 94 °C for 30 s, annealing at 55 °C for 30 s, and extension at 72 °C for 2 min and final extension at 72 °C for 5 min. In the second round of PCR, five sets of primers (SR1-SR9, SR4-SR12, SR8-25F1R, SR12cF-25R1 and LSU D1R-LSU R2; Takano and Horiguchi 2006) were used with PCR mixtures of KOD-Plus-Ver. 2 Kit (Toyobo, Osaka, Japan), 0.5 μl of the first round PCR product as the DNA template, and the same PCR conditions except for extension at 72 °C for 1 min. In the third round of PCR, five sets of primers (SR-1c-SR5, SR4-SR9, SR8-SR12, LSU D1R-25R1 and LSU D3A-LSU R2; Takano and Horiguchi 2006) were used with PCR mixtures of the TaKaRa EX taq system (Takara Bio Inc., Shiga, Japan), 0.5 μl of the second round PCR products as the DNA template, and the same PCR conditions except for extension at 72 °C for 30 s. PCR products were sequenced directly using the ABI PRISM BigDye Terminator Cycle Sequencing Kit (Perkin-Elmer, Foster City, CA). These techniques are modifications of the methods described by Takano and Horiguchi (2006).

Single-cell PCR amplification and sequencing of cells of *Archaeperidinium minutum*

Motile cells of *A. minutum* were isolated from plankton net samples for single cell-PCR analysis (SSU) from surface waters off Nagayo, Japan and off Mie, Japan and for single-cell PCR analysis (LSU) from surface waters off Sasebo, Japan (Table 1). SSU and partial LSU (D1-D2) rDNA sequences were amplified from a single motile cell with the appropriate primer sets following a procedure used previously by Matsuoka et al. (2009). After microscope observations, each motile cell was collapsed with a sharp glass rod and its contents were transferred to a 200-μl tube containing 10 μl distilled water. PCR amplification was carried out within a 20-μl reaction volume according to the manufacturer's recommendation for KOD-Plus-DNA Polymerase (Toyobo, Osaka, Japan) on a GeneAmp 9600 PCR System (Perkin-Elmer, Foster City, CA). SSU rDNA was amplified using primers previously reported (Kawami et al. 2006; Matsuoka et al. 2006; Nakayama et al. 1996). PCR was performed in two steps. The first round of PCR consisted of an initial denaturation at 95 °C for 10 min, followed by 35 cycles at 95 °C for 1 min, 55 °C for 1 min, and 72 °C for 3 min. The reaction was completed with a final elongation at 72 °C for 10 min. The primer pair used in the first round of PCR to amplify the full length SSU rDNA was SR1 and SR12 (Nakayama et al. 1996). The second round of PCR consisted of an initial denaturation at 95 °C for 10 min, followed by 40 cycles at 94 °C for 30 s, 55 °C for 30 s, and 72 °C for 30 s. The reaction was completed with a final elongation at 72 °C for 10 min. The product of the first round of PCR was used as a template for the second round, where the following combinations of primer pairs were used: SR1 and SR5kaw, SR4 and SR9, and SR8kaw and SR12 (Matsuoka et al. 2006). The PCR product was purified using a Microcon YM-100 Centrifugal Filter Device (Millipore, Billerica, MA), and the cycle-sequencing reaction was performed using an ABI PRISM BigDye™ Terminator v3.1 Cycle Sequencing Kit (Perkin-Elmer) following the manufacturer's protocol. Sequencing was run on an ABI PRISM 377 Sequencer (Perkin-Elmer) with the PCR primer set and internal primers.

Sequence alignments and phylogenetic analyses

SSU and LSU rDNA sequences were aligned using MacClade 4 (Maddison and Maddison 2000) based on the datasets of Mertens et al. (2012a). The final alignment of the SSU rDNA dataset consisted of 72 taxa and contained 1,434 base pairs for *P. fukuyoi*. The outgroup species was the alveolate protist *Perkinsus marinus*. The final alignment of the LSU rDNA dataset consisted of 65 taxa and contained 483 base pairs for *P. fukuyoi*, whose region included the domains D1–D6, excluding the hypervariable part of domain D2. The apicomplexan *Neospora caninum* was used as the outgroup. The alignments are available from the authors upon request. Phylogenetic trees for SSU and LSU rDNA were constructed using maximum likelihood (ML) and Bayesian analysis, respectively. For ML, the alignments were analyzed by GARLI version 0.951 (Zwickl 2006). The TIM2 + I + G substitution model was selected by the Akaike information criterion as implemented in jModelTest 0.1.1. (Posada 2008). The parameters were as follows: assumed nucleotide frequencies are A = 0.2571, C = 0.1956, G = 0.2466, T = 0.3007; substitution rate matrix with A–C substitutions = 1.4987, A–G = 4.7492, A–T = 1.4987, C–G = 1.0000, C–T = 9.1256, G–T = 1.0000; proportion of sites assumed to be invariable = 0.1960 and rates for variable sites assumed to follow a gamma distribution with shape parameter = 0.5460. For the LSU rDNA dataset, the TIM2 + G model of nucleotide substitution with a gamma-distributed rate of variation across sites was chosen. The parameters were as follows: assumed nucleotide frequencies are A = 0.2657, C = 0.1777, G = 0.2977, T = 0.2590; substitution rate matrix with A–C substitutions = 1.3814, A–G = 3.5160, A–T = 1.3814, C–G = 1.0000, C–T = 10.6670, G–T = 1.0000; rates for variable sites assumed to follow a gamma distribution with shape parameter = 0.5410. Bootstrap analyses for both datasets were carried out for ML with 100 replicates to evaluate statistical reliability. MrBayes version

3.1.2 was used to perform Bayesian analyses on both SSU and LSU rDNA datasets (Huelsenbeck and Ronquist 2001). The evolutionary model used in Bayesian analyses for the SSU rDNA dataset was the GTR model with gamma-distributed rate variation across sites and a proportion of invariable sites, and the GTR model with a gamma distribution for the LSU rDNA dataset. The program was set to operate four Monte-Carlo-Markov chains starting from a random tree. A total of 7,500,000 generations (SSU) and 4,000,000 generations (LSU) were calculated with trees sampled every 100 generations. The first 18,750 (SSU) and 10,000 (LSU) trees in each run were discarded as burn-in. Posterior probabilities (PP) correspond to the frequency at which a given node was found in the post-burn-in trees.

RESULTS

Results of germination experiments

Undescribed motile cells, here assigned to *P. fukuyoi* n. sp., emerged from round brown spiny cysts isolated from surface sediments of Brentwood Bay, Saanich Inlet (four specimens identified), Strait of Georgia (one specimen identified) and from San Pedro Harbor, California (four specimens identified) (Table 1 and Fig. S1). After 1 or 2 d of incubation, motile cells germinated from the cysts. These cells died a few days after germination and never divided.

None of the 173 specimens of *I. minutum* from Barrow Strait, northern Canada germinated. However, a preliminary report of the cyst–theca relationship has been described (Rochon and Potvin 2006).

Species descriptions.

Division DINOFLAGELLATA (Bütschli 1885) Fensome et al. 1993
Class DINOPHYCEAE Pascher 1914
Subclass PERIDINIPHYCIDAE Fensome et al. 1993
Order PERIDINIALES Haeckel 1894
Family PROTOPERIDINIACEAE Balech 1988 nom. cons.
Subfamily PROTOPERIDINIOIDEAE (Autonym)
Genus *Protoperidinium* Bergh 1881

Protoperidinium fukuyoi *Mertens, Head, Pospelova et Matsuoka n. sp. (Fig. 1–54)*

Diagnosis. A small species of the genus *Protoperidinium* with the tabulation formula Po, X, 4′, 3a, 7″, 4c, 6s, 5‴, 2⁗. The motile cell is slightly ovoidal in equatorial view and approximately circular in polar view, with a low apical horn and no antapical extensions. Plate 1′ is ortho-type, 1a is penta-type, and 2a and 3a are hexa-type. Plates are smooth with scattered trichocyst pores. The cyst is spherical to subspherical and light brown to golden brown in colour. Cell contents are typically colourless. The cyst surface is smooth to finely and faintly granulate, bearing numerous erect, flattened, straight to curved processes that taper to acuminate or blunt tips. Processes are typically clustered in straight or arcuate linear complexes, but some are distributed irregularly over the entire cyst. The archeopyle is angular, apical, and saphopylic, comprising release of plates Po, X, 2′, 3′ and 4′.

Etymology. The specific epithet honours Dr. Yasuwo Fukuyo for his significant taxonomic research on marine dinoflagellates and their cysts.

Type locality. Brentwood Bay, Saanich Inlet, British Columbia, Canada (48.57°N, 123.47°W, 5 m water depth).

Gene sequence. The SSU and LSU rDNA gene sequence of the cyst—GenBank accession no. AB780842 (SSU) and AB780844 (LSU).

Holotype. Fig. 1–15.

Description. *Description of motile cell of P. fukuyoi* (Fig. 1–20). The excysted motile cells (five observed and not preserved) were slightly ovoidal with a short apical horn and no antapical extensions (Fig. 1). The cell contents were colourless. The nucleus was located on the dorsal side of the epitheca. The thin and smooth thecal plates carried randomly arranged trichocyst pores on the surface.

The plate arrangement on the epitheca was more-or-less bilaterally symmetrical, except for the relatively large 3″ and small 2″ and the asymmetrical arrangement of three anterior intercalary plates. The oval apical pore plate (Po) was surrounded by a very low apical collar formed by the raised edges of the plates 2′, 3′ and 4′ (Fig. 7). The canal plate (X) was elongate and rectangular (Fig. 2). The first apical plate (1′) was rhombic (ortho-type) and the sides of plate 1′ contacting plates 2′ and 4′ were shorter than those contacting plates 1″ and 7″ (Fig. 2). Plates 2′ and 4′ were pentagonal (Fig. 5, 7) and plate 3′ was irregularly quadrangular (Fig. 6). The three anterior intercalary plates were unequal in size (Fig. 5–7). The first anterior intercalary plate (1a) was the smallest, pentagonal and located on the left lateral surface of the epitheca (Fig. 5). The second anterior intercalary plate (2a) was hexagonal and of intermediate size, and located on the left dorsal surface of the epitheca (Fig. 6, 7). The third anterior intercalary plate (3a) was also hexagonal and slightly larger than 2a, and located on the right dorsal surface of the epitheca (Fig. 6, 7). The precingular series consisted of seven plates. Plates 1″ and 7″ were hexagonal (Fig. 3), plates 3″, 4″ and 6″ pentagonal (Fig. 4, 5, 7, 14), and 2″ and 5″ quadrangular (Fig. 3, 14). The cingulum was slightly left-handed (descending), lined with narrow lists and comprising four cingular plates (Fig. 3, 4). There was no transitional plate (t) (Fig. 13). Plate 1c was longer than plate 1″, and nearly reached the middle of 2″ (Fig. 3). Plate 2c was the longest of the series and reached a short way beyond the 4″/5″ boundary and almost to the 3‴/4‴ boundary (Fig. 14, 15). Plate 3c was of median length reaching almost to the 6″/7″ boundary (Fig. 4, 15) and plate 4c was similar in size to plate 1c.

The sulcus was flat and consisted of four large plates and two smaller plates. The anterior sulcal plate (Sa) was relatively elongate and its anterior part intruded between plates 1″ and 7″, narrowly contacting 1′ (Fig. 13). The right

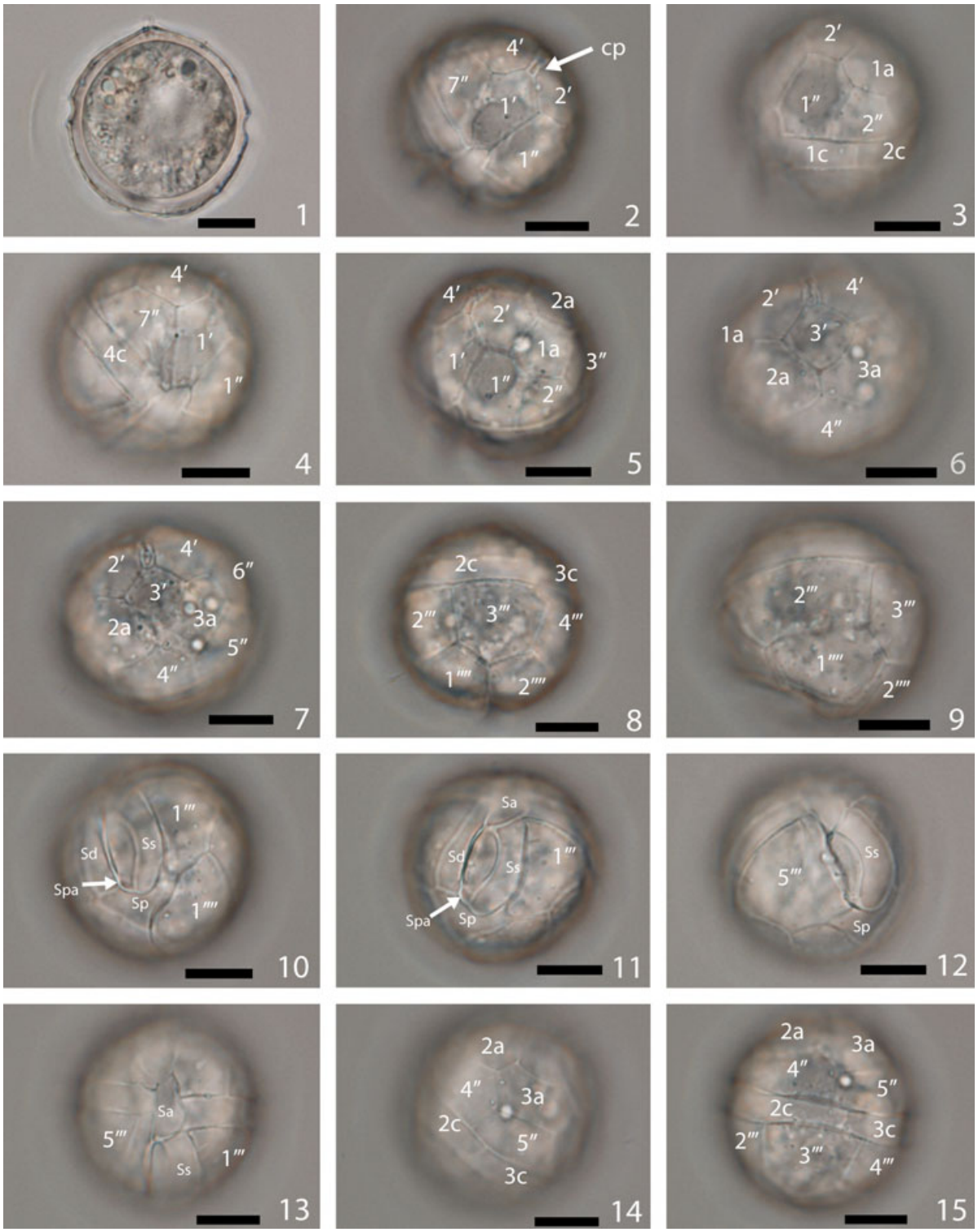

Figure 1–15 Holotype of *Protoperidinium fukuyoi* n. sp. after germination of a cyst (KATF2) from Brentwood Bay, Saanich Inlet, BC [Photos K.N.M.]. **1**. Cross-section in equatorial view showing general shape. **2**. Ventral view showing asymmetrical rhombic 1′ and arrow indicating canal plate (cp). **3**. Ventral view showing pentagonal 1‴ and quadrangular 2‴. **4**. Ventral view showing hexagonal 7″. **5**. View of ventral surface of epitheca showing arrangement of 1a and surrounding plates. **6,7**. View of epitheca showing dorsal surface and arrangement of 2a and 3a. **8,9**. View of dorsal surface of hypotheca showing pentagonal 3‴ and position of 2c vs. 3c and arrangement of antapical plates. **10**–**12**. Arrangement of sulcal plates and surrounding plates. **13**. Ventral view showing anterior sulcal plate (Sa). **14,15**. View of dorsal surface showing arrangement of plates. All scale bars = 10 μm. Sulcal plates as follows: Sa, anterior sulcal; Sd, right sulcal; Sp, posterior sulcal; Ss, left sulcal.

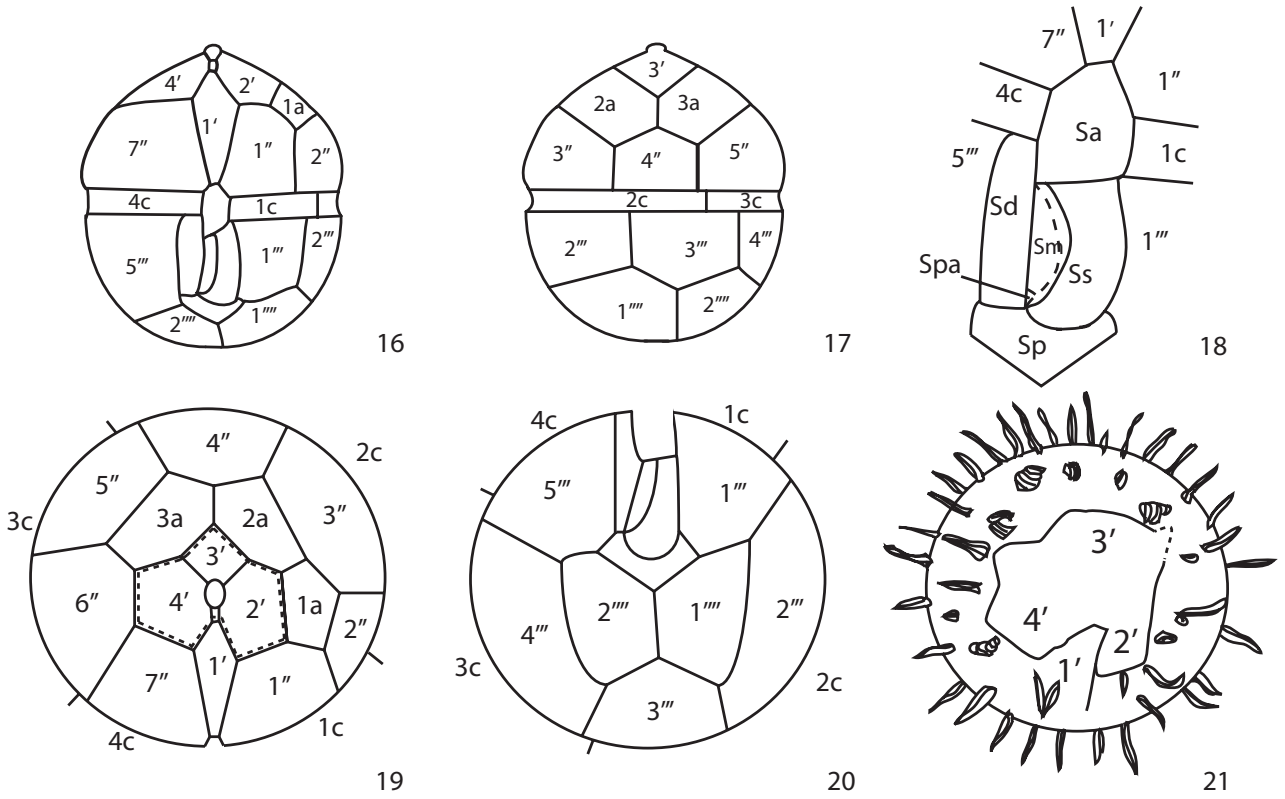

Figure 16–21 Interpreted tabulation of *Protoperidinium fukuyoi* n. sp. **16**. Ventral surface. **17.** Dorsal surface. **18**. Sulcal plates. **19**. Epitheca, with a dashed line representing the principal archeopyle suture on the cyst. **20**. Hypotheca. Sulcal plates as follows: Sa = anterior sulcal; Ss = left sulcal; Sm = median sulcal (=ventral pore region); Sd = right sulcal; Spa = additional posterior sulcal; Sa = posterior sulcal. **21**. Schematic drawing of cyst, with the principal archeopyle suture based on a tracing of the specimen shown in Fig. 44–48.

sulcal plate (Sd) reached the cingulum (Fig. 11). A small sulcal wing was connected to the left side of the Sd plate, next to the median sulcal plate (Sm) and the additional posterior sulcal plate (Spa) (Fig. 10–12). The left sulcal plate (Ss) was long and formed a J-shaped curve (Fig. 10–12), its anterior margin broadly connecting with the Sa plate and barely (Fig. 13) or nearly (Fig. 18) touching plate 1c. The posterior sulcal plate (Sp) was large and asymmetrically V-shaped (Fig. 10, 11).

The plate arrangement of the hypotheca was also mostly symmetrical, featuring five postcingular plates. Plate 5‴ was wider than plate 1‴. Plates 1‴, 3‴, and 5‴ were pentagonal, and 2‴ and 4‴ were quadrangular (Fig. 8–12). The antapical series comprised two plates, 1⁗ and 2⁗ (Fig. 8, 9).

The plate formula is thus Po, X, 4′, 3a, 7″, 4c, 6s, 5‴, 2⁗, and the complete tabulation is illustrated in Fig. 16–20.

Description of cyst of P. fukuyoi (Fig. 21–54). Cysts were small and proximochorate, light brown to golden brown in colour, with a spherical to subspherical central body bearing numerous processes (Fig. 21–48). Living cysts contained abundant colourless granules (Fig. 24). The central body wall was thin (> 0.3 μm) and unstratified under light microscopy, with a smooth to finely and faintly granulate surface (Fig. 54). Processes were narrow (up to ~1.5 μm at their base), erect, and non-branching, gradually tapering to blunt or (more frequently) acuminate tips (Fig. 22–48). Individual processes appeared to be hollow with circular bases, distally becoming flattened and blade-like. Processes were typically grouped into clusters, adjacent processes in each cluster fused at their bases and often for much, or most, of their length, although process tips were typically free (Fig. 24). Process clusters were often arranged into straight or curved lineations up to ~7 μm in length at their base, with the fusion of adjacent processes creating a striated appearance along the length of each process cluster under LM. The degree of process clustering varied between cysts but all cysts had some process clusters. Process distribution was non-tabular and irregular, with processes covering the entire cyst including the operculum (Fig. 34–42). Process length was fairly constant for individual specimens. Occasional scattered, isolated hair-like processes up to about 0.3 μm in diameter were also present (Fig. 34, 45, 54). The archeopyle was angular, apical, and saphopylic, involving release of plates 2′, 3′ 4′. On one specimen (Fig. 21, 44), the Po plate and x (canal) plate were also released, as indicated by the truncated anterior margin of 1′, and this was assumed to be the usual configuration. Although we did not observe the operculum disintegrate into separate plates, we observed

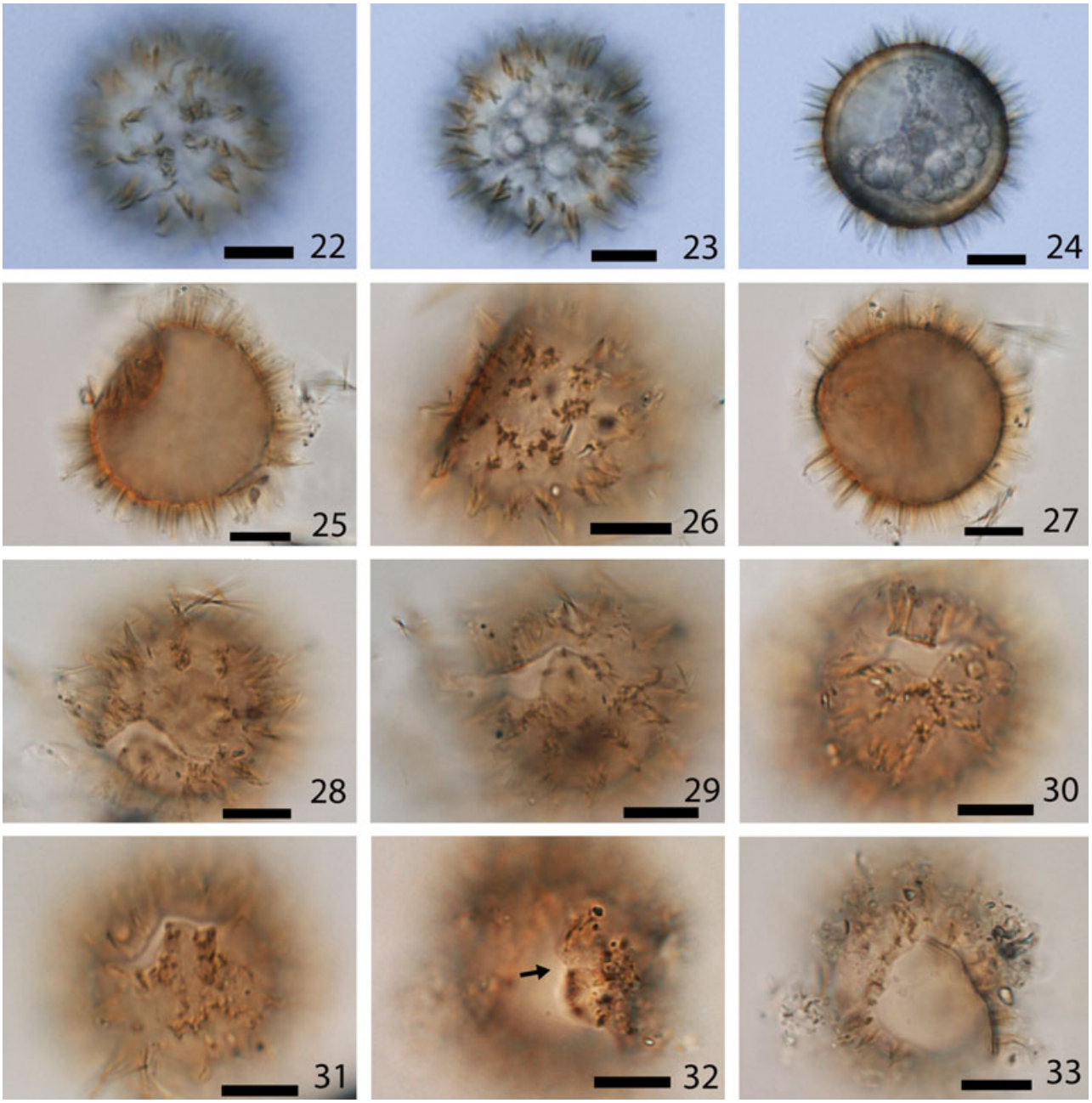

Figure 22–33 Light microscope photos of cysts of *Protoperidinium fukuyoi* n. sp. from Saanich Inlet, BC [Photos K.N.M.]. **22–24**. Progressively lower foci through a cyst with cell content including colourless granules from Brentwood Bay, Saanich Inlet, isolated for PCR analysis (KC64). **25–31**. Germinated cyst from culture (Brentwood Bay, KATF2) which gave rise to the thecate stage depicted in Fig. 1–15, showing typical process bases and a compound polyplacoid apical archeopyle. The cyst has been rotated to show different views of the archeopyle. **32–33**. Germinated cyst from a different incubation experiment (SA1E12) from central Saanich Inlet showing the opened operculum in upper and lower focus. Arrow denotes presence of suture line in operculum in Fig. 32. All scale bars = 10 μm.

sutures between the apical plates of the operculum, suggesting that apical plates were released separately (Fig. 32, 38). The anterior margin of plate 1′ was expressed along the archeopyle margin as a triangular protrusion, its apex truncated by contact with the X plate, as discussed above (Fig. 21, 44). A tracing of the archeopyle is shown in Fig. 21 and corresponding thecal plate boundaries by dashed lines in Fig. 19. No accessory sutures were observed. In specimens recovered from sediments, the archeopyle was usually distorted by folding and crumpling of the thin-walled central body, but some traces were usually visible. No other expression of tabula-

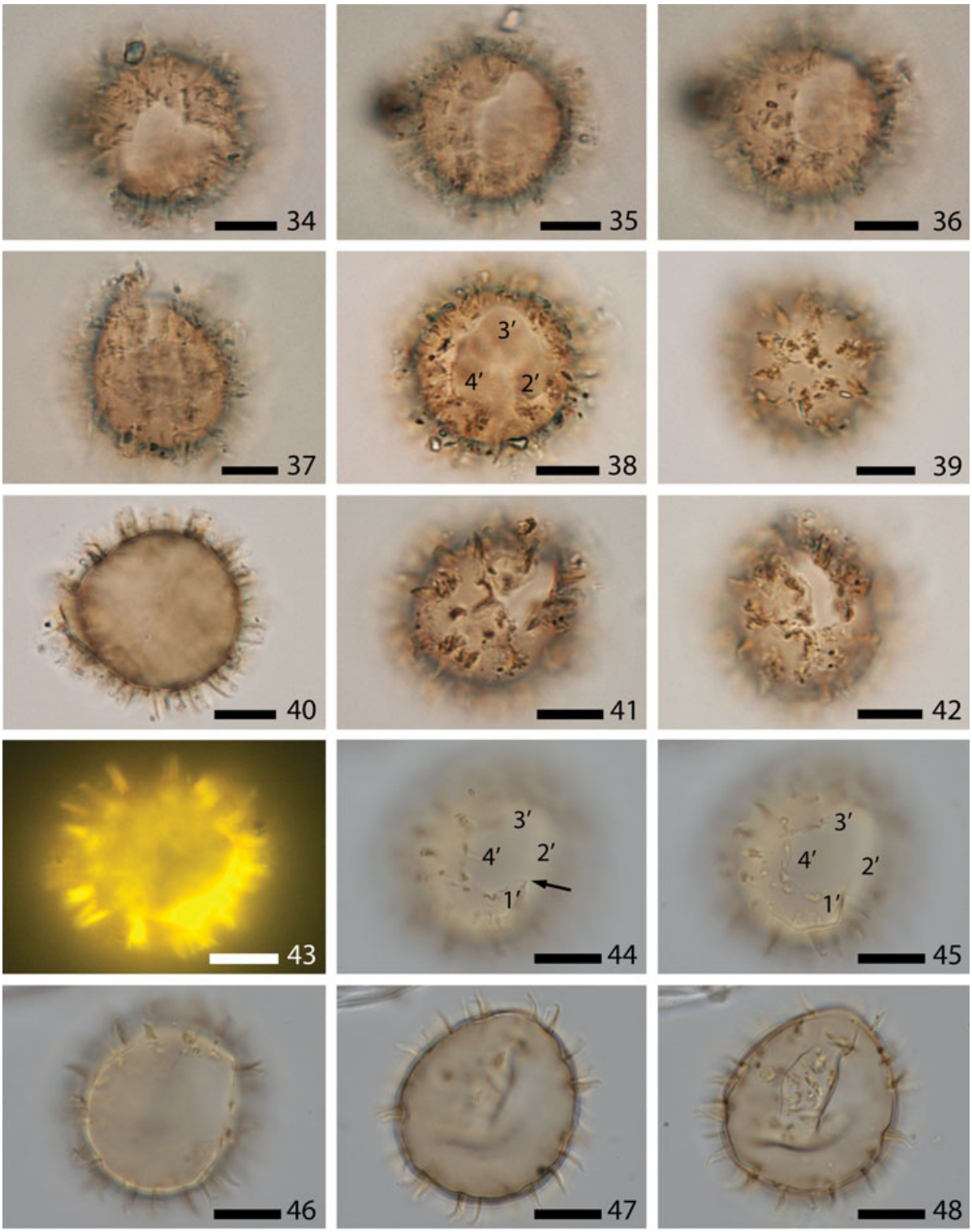

Figure 34–48 Light microscope photos of cysts of *Protoperidinium fukuyoi* n. sp. from various locations [Photos 34–43 K.N.M.; 44–48 M.J.H.]. **34–39**. Cysts germinated from San Pedro Harbor. **34–37** Different orientations of one specimen (SPH3A1). **38.** Specimen (SPH2H4) showing the polyplacoid operculum. **39–43**. SPHE2. **43**. Autofluorescence of cyst. **44–48**. Cyst processed palynologically from sediment, in apical view at progressively lower foci showing the archeopyle formed by loss of plates 2′–4′ as well as the Po and X (canal) plate; with an arrow (Fig. 46) indicating the truncated anterior margin of 1′ that would have adjoined the X plate. Fig. 48 shows the distinctive clustering of processes. UVic 04-203 (SBB893 A,B), 1H-1, 3–4 cm, RB Depth mbsf 0.24 m, slide 1, England Finder reference K50/0 (label left), Age 0.01 ka. Ocean Drilling Program (ODP) Leg 146 Hole 893A (Santa Barbara Basin). All scale bars = 10 μm.

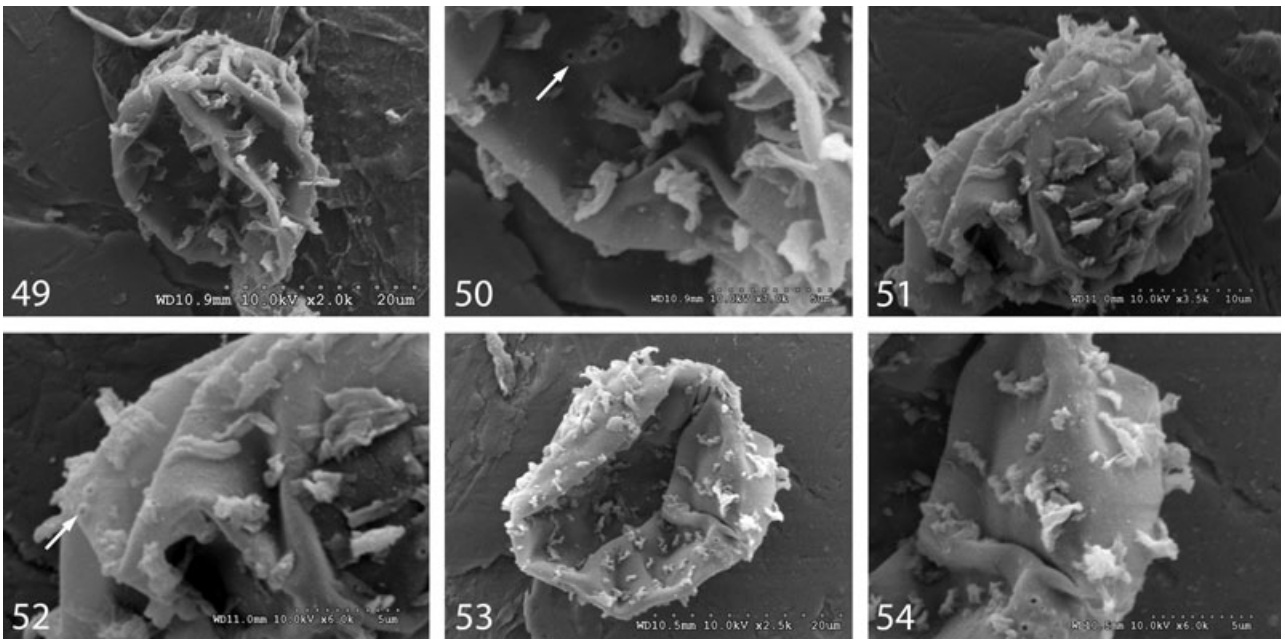

Figure 49–54 SEM photos of cysts of Protoperidinium fukuyoi n. sp. from Strait of Georgia CM3 sediment trap. [Photos V.P.] **49.** Specimen with many clusters of processes. **50.** Detail of Fig. 49. **51.** Slightly crushed specimen. **52.** Detail of Fig. 51. Arrows in Fig. 50 and 52 show raised circular pits that appear to represent the broken bases of individual processes. **53.** Specimen with reduced processes. **54.** Detail of Fig. 53 showing fused processes and finely granulate surface.

tion was seen. The description is based on cysts used in the incubation experiments and those recovered from sediment and prepared using palynological methods, with no differences between these cysts being observed.

Dimensions. Incubated motile cells: length, 29.0 (30.6) 32.4 μm (SD = 1.7, *n* = 3); width, 27.0 (28.4) 30.0 μm (SD = 1.5, *n* = 3). Three cells were measured.

Cysts germinated to give identifiable thecae: central body maximum diameter, 23.8 (27.2) 31.3 μm (*n* = 12), and minimum diameter, 23.1 (26.9) 31.0 μm (*n* = 12); average length of five processes per cyst, 4.2 (5.1) 6.6 μm (*n* = 60). Twelve cysts were measured.

Cysts palynologically prepared from surface sediments of different locations: central body maximum diameter, 23.0 (28.0) 34.6 μm (*n* = 21), and minimum diameter, 24.5 (27.9) 33.3 μm (*n* = 21); average length of five processes per cyst, 1.9 (4.3) 7.4 μm (*n* = 90). Twenty-one cysts were measured.

Comments. Cysts of *P. fukuyoi* have been described as cyst type A by: Pospelova et al. (2006, supplementary plates, plate 3, fig. 8), Radi et al. (2007, not illustrated), Pospelova et al. (2008, not illustrated), Pospelova et al. (2010, p. 28, plate VI, fig. 5), Krepakevich and Pospelova (2010, p. 1931, plate 3, fig. i,j), Price and Pospelova (2011, p. 10, plate IV, fig. 6) and Bringué et al. (2013, plate 1, fig. 10).

The geological preservability of these cysts was demonstrated by their ability to withstand palynological treatment, and presence in sediments at least as old as 39 ^{14}C ka BP (Pospelova et al. 2006).

Genus *Islandinium* Head, Harland & Matthiessen 2001

***Islandinium minutum* (Harland & Reid *in* Harland et al. 1980) Head, Harland & Matthiessen 2001 (Fig. 55–66)**

Comments. Three cysts with very similar morphology and corresponding to *I. minutum* as described by Head et al. (2001) were isolated for single-cyst PCR (Fig. 55–66). Cysts were collected from surface sediments of Barrow Strait, Nunavut, Canada (Fig. S1). All cysts possessed a granulate central body surface bearing non-tabular, erect, acuminate processes that were solid to apiculocavate. The archeopyle could not be observed on encysted specimens. The three cysts had a central body maximum diameter, 37.1 (39.2) 41.7 μm (SD = 2.3), minimum diameter, 36.8 (38.6) 41.1 μm (SD = 2.2), process length 4.7 (5.4) 6.1 μm (SD = 0.5).

Phylogenetic position of *P. fukuyoi,* Japanese *A. minutum* and *I. minutum* as inferred from rDNA sequences

SSU rDNA

We obtained 1,736 base pairs from three cysts of *P. fukuyoi* isolated from Brentwood Bay, Saanich Inlet (accession number: AB780842) which were identical, 1,734 base pairs from three specimens of *I. minutum* (accession number: AB780843) which were also identical, 1,758 base pairs from one motile cell of *A. minutum* from off Nagayo, Japan (accession number: AB780999) and 1,768 base pairs from one motile cell of *A. minutum* from off Mie, Japan (accession number: AB781000). These sequences were used for the phylogenetic analyses (Fig. 67).

Protoperidinium fukuyoi and *I. minutum* form a clade with *P. fusiforme*, *P. americanum*, *P. parthenopes* and *P.*

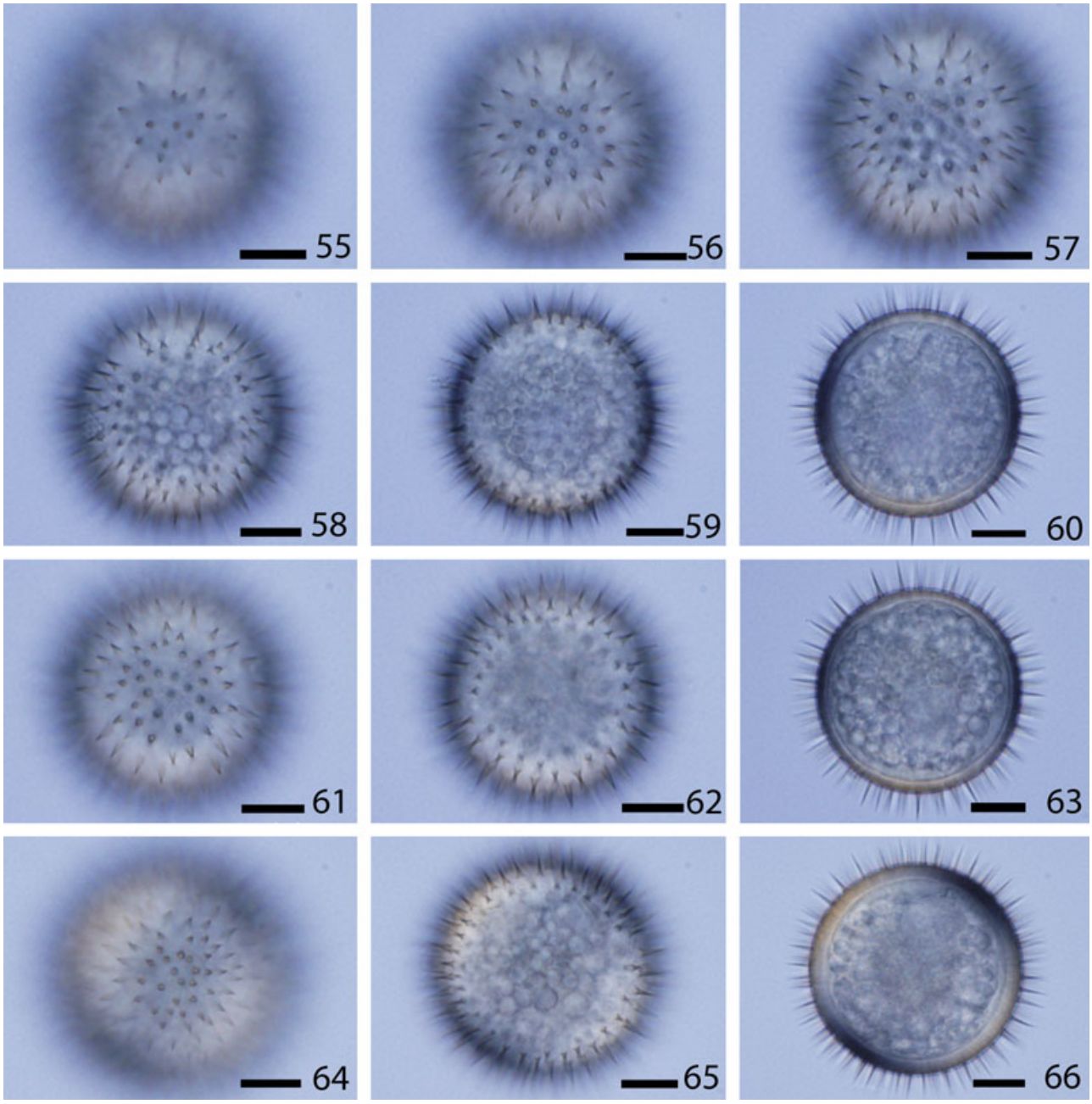

Figure 55–66 Specimens of *Islandinium minutum* isolated from Barrow Strait, Nunavik, Canada for single-cyst PCR [Photos Y.T.]. **55–60.** Specimen 1(KC23), **61–63**. Specimen 2 (KC22), **64–66.** Specimen 3 (KC24). Note the granulate central body surface, and dense distribution of solid to apiculocavate processes that taper to fine points. All scale bars = 10 μm.

tricingulatum (< 50% ML bootstrap support and 1.00 Bayesian PP; Fig. 67). In this clade, *P. fukuyoi*, *P. fusiforme*, *P. parthenopes* and *P. americanum* formed a clade with 100% ML bootstrap support and 1.00 Bayesian PP. *Protoperidinium tricingulatum* and *I. minutum* are positioned at the base of this clade. The Japanese specimens of *A. minutum* formed a clade with other strains of *A. minutum* and *A. saanichi* (the *Minutum* subgroup sensu Matsuoka and Kawami in press). Four other well-supported clades comprising members of the Protoperidiniaceae were also revealed: *Protoperidinium* sensu stricto clade, *Oceanica* clade, *Diplopsalopsis* clade, and the *Monovelum* subgroup (Fig. 67). The names of these clades are used in Matsuoka and Kawami (in press).

LSU rDNA

We obtained 1,203 base pairs from one cyst of *P. fukuyoi* isolated from Brentwood Bay, Saanich Inlet (accession number: AB780844) and 1,433 base pairs from one motile cell of *A. minutum* from off Sasebo, Japan (accession

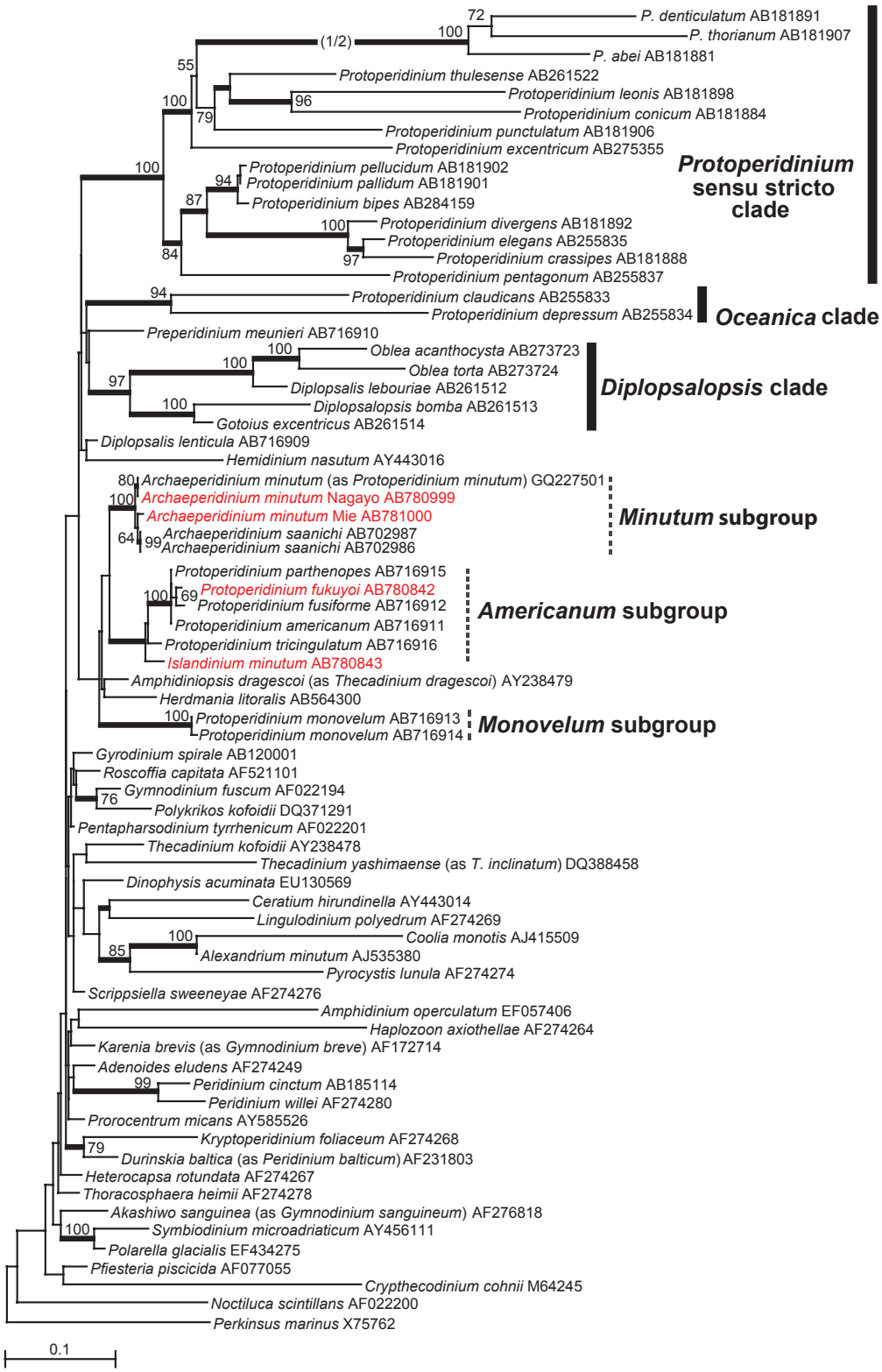

Figure 67 Maximum-likelihood (ML) tree of dinoflagellates inferred from SSU rDNA sequences, based on new sequence data for *Archaeperidinium minutum* from Mie and Nagayo (Japan), *Protoperidinium fukuyoi* n. sp., and *Islandinium minutum.* ML bootstrap support values over 50% are shown. Thick branches indicate Bayesian posterior probabilities (PP) over 0.95. Clades are labelled and marked with vertical lines on the right, with dashed lines indicating subgroups of the *Monovela* group. The scale bar represents inferred evolutionary distance in changes/site. The branch leading to fast-evolving species has been halved (indicated by 1/2).

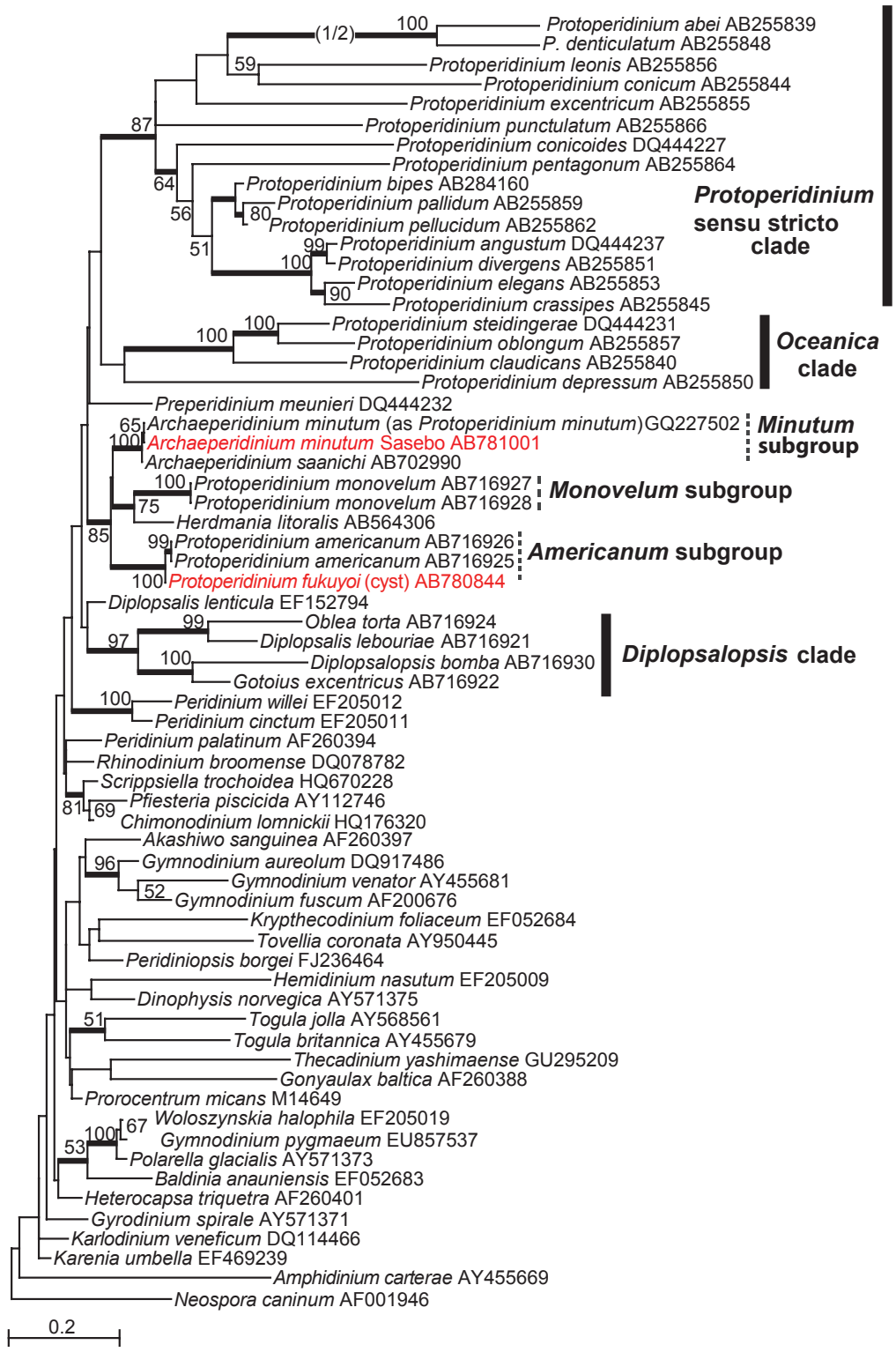

Figure 68 Maximum-likelihood tree inferred from LSU rDNA sequences based on new sequence data for *Archaeperidinium minutum* from Sasebo, Japan and *Protoperidinium fukuyoi* n. sp. ML bootstrap support values (ML) over 50 and Bayesian posterior probabilities (PP) over 0.95 are shown at the nodes (ML/PP). Clades are labelled and marked with vertical lines on the right, with dashed lines indicating subgroups of the *Monovela* group. The scale bar represents inferred evolutionary distance in changes/site. The branch leading to fast-evolving species has been halved (indicated by 1/2).

number: AB781001), and these sequences were used for the phylogenetic analyses (Fig. 68). As with the results of ML and Bayesian analyses, *P. fukuyoi* and two sequences of *P. americanum* formed a clade (*Americanum* subgroup). *Protoperidinium monovelum* formed a separate clade and *Herdmania litoralis* was positioned at the base of this clade (*Monovelum* subgroup). Again, a third clade was formed by *A. minutum* and *A. saanichi* (*Minutum* subgroup). These three clades formed one clade with 85% ML bootstrap support and 1.00 Bayesian PP. The other members of the Protoperidiniaceae formed three clades; the *Protoperidinium* sensu stricto clade, *Oceanica* clade, and the *Diplopsalopsis* clade. These clade names are also used in Matsuoka and Kawami (in press).

Recent distribution of cysts of *P. fukuyoi,* inferred ecology and biostratigraphy

Cysts of *P. fukuyoi* were recorded in the surface sediments from the coastal region of British Columbia, Gulf of California and along the California and Mexico coasts (Table S1 and Fig. S1). The highest abundance of *P. fukuyoi* cysts was recorded in surface sediments of the Strait of Georgia where the cysts contribute up to 4.8% of the cyst assemblages (Radi et al. 2007). The highest cyst concentration (up to 893 cysts/g) was recorded in surface sediments of coastal California (Pospelova et al. 2008).

Cysts of *P. fukuyoi* were found in surface sediment samples corresponding to August SSTs of ~12–31 °C, and February SSTs of ~6–28 °C. Sea-surface salinities had a range of 17–35 psu (August) and 23–35 psu (February). Annual MODIS primary productivity ranged from 150 to 630 g C m^2/yr.

Sediment traps in the Strait of Georgia (Pospelova et al. 2010), Saanich Inlet (Price and Pospelova 2011) and the Santa Barbara Basin (Bringué et al. 2013) recorded optimum conditions during summer with SSTs of ~14–18 °C and SSSs of 22–34 psu. All sites in the northeastern Pacific were free of sea-ice.

We also observed cysts of *P. fukuyoi* in marine isotope stages 1–3 (late Quaternary) of the Santa Barbara Basin (ODP core SBB983A, down to ~39 ^{14}C ka) and the Guaymas Basin (MD02-2515, down to ~39 ^{14}C ka), as well as in recent sediments from the Strait of Georgia (CM3 core, down to ~20 yr) (Table S1 and Fig. S1).

DISCUSSION

Comparison based on theca

Five other species that belong to the *Monovela* group of Abé (1936, 1981) have three anterior intercalary plates: *Protoperidinium asymmetricum* (Abé 1927) Balech 1974; *Protoperidinium bolmonense* Chomérat & Couté 2008; *P. monovelum* (Abé 1936) Balech 1974; *P. parthenopes* Zingone & Montresor 1988 and *Protoperidinium vorax* Siano & Montresor 2005.

Protoperidinium vorax differs in its smaller size (16–26 μm), an elongated 2a plate that contacts 2″, a smaller wing, and only five sulcal plates. *Protoperidinium bolmonense* is also smaller (18–22 μm), has an elongated 2a plate and probably (as indicated by the authors) has only four sulcal plates. *Protoperidinium parthenopes* is of similar size, but has differently shaped anterior intercalary plates. *Protoperidinium asymmetricum* has a distinct straight diagonal suture on the epitheca that divides plates 1a, 2′ and 4′ from plates 2a, 3′ and 3a, a feature not present in *P. fukuyoi* n. sp.

Comparison based on cyst

The distinctive shape of processes and their clustering into straight or arcuate linear complexes, and the saphopylic archeopyle formed by release of three apical plates and Po and X plates, distinguishes this species from all other round brown spiny cysts. This cyst was reported previously as cyst type A in palynological preparations from a core off southern California (Pospelova et al. 2006) and the Guaymas Basin (Price et al. 2013), from surface sediments of the northeastern Pacific (Krepakevich and Pospelova 2010; Limoges et al. 2010; Pospelova et al. 2008; Radi et al. 2007) and from sediment traps in coastal waters of British Colombia (Pospelova et al. 2010; Price and Pospelova 2011). Cyst morphology, most notably the nontabular process distribution and archeopyle resulting from the loss of three apical plates and Po and X plates, is fully encompassed within the cyst-defined genus *Islandinium*. However, as the thecal affinity of *Islandinium* is unknown, whereas that of our new species is well documented, we consider placement in the motile-stage-defined genus *Protoperidinium* presently more appropriate, pending future detailed studies of both *Protoperidinium* and *Islandinium*.

Classification of the *Monovela* group

The *Monovela* group was erected to accommodate *Protoperidinium* species with or without an apical horn, no antapical horns/spines, a flat ventral area (flat sulcus and a sulcal fin positioned at the left suture of the right sulcal plate) and a plate formula of 4′, 2a–3a, 7″, 5‴, 2⁗ (Abé 1936; p. 669–670). Three subgroups within the *Monovela* group were recognized by Matsuoka and Kawami (in press) on the basis of thecal morphology and molecular phylogenetic data: the *Americanum*, *Minutum* and *Monovelum* subgroups. The molecular phylogenies constructed here show that *P. fukuyoi* n. sp. and *I. minutum* belong to the *Americanum* subgroup, and that the Japanese specimens of *A. minutum* belong to the *Minutum* subgroup. The cysts and thecae have a number of traits that can be used to distinguish those species within the *Americanum* subgroup from species of other subgroups. These are outlined in Table 2. Several additional species (*P. asymmetricum* (Abé 1927) Balech 1974; *P. bolmonense* Chomérat & Couté 2008; *P. vorax* Siano & Montresor 2005; *Protoperidinium mutsuense* (Abé 1936) Balech 1974 (see Mertens et al. 2012a p. 56–59 for discussion of other species presumably related to the *Minutum* subgroup) are likely closely related to the *Monovela* group, but as cyst

Table 2. Comparison between different species within the subgroups of the *Monovela* group

Subgroup	Species name	Sulcal plates	Anterior intercalary plates	Cingular plates	Apical pore plate	Theca texture	Cyst	Cyst archeopyle	Ref
Americanum	*Protoperidinium tricingulatum*	6	2	3c	Low collar, square	S	Y	2′-4′ + Po + X, THER	(1)
Americanum	*Protoperidinium americanum*	**7**	4	4c	Low collar, elongated	S	Y	2′-4′ + Po + X, SAP	(2)
Americanum	*Protoperidinium parthenopes*	6	3	4c	Low collar, elongated	S	Y	2′-4′ + Po + X, SAP	(3)
Americanum	*Protoperidinium fukuyoi*	6	3	4c	Low collar, elongated	S	Y	2′-4′ + Po + X, SAP	This study
Americanum	*Protoperidinium fusiforme*	?	2	4c	Low collar, elongated	S	NA	?	(4)
Americanum	*Islandinium minutum*	NA	NA	NA	NA	NA	Y	2′-4′ + Po + X, SAP	(5)
Monovelum	*Protoperidinium monovelum*	5	3	4c	Low collar, elongated	G	NA	?	(6)
Minutum	*Archaeperidinium minutum* sensu (7)	6?	2	3c+t	High collar, elongated	M	Y	2a, THER	(7)
Minutum	*A. minutum* sensu (8)	NA	2	3c+t	High collar, elongated	M	Y	2a, THER	(8)
Minutum	*Archaeperidinium saanichi*	6	2	3c+t	High collar, elongated	M	Y	2a, THER	(9)

1 = Kawami et al. (2009); 2 = Lewis and Dodge (1987); 3 = Kawami and Matsuoka (2009); 4 = Abé (1981); 5 = Head et al. (2001); 6 = Abé (1936); 7 = Ribeiro et al. (2010); 8 = Yamaguchi et al. (2011); 9 = Mertens et al. (2012a).
NA = not acknowledged; S = smooth; G = granulate; M = microreticulate; THER = theropylic; SAP = saphopylic; Po = pore plate; X = canal plate.

information and molecular data are not available for these species, they are not included here.

Comparative morphology of motile stages within the Monovela group.

Species of the *Americanum* subgroup have three to four cingular plates and no transitional plate (t). *Protoperidinium monovelum* of the *Monovelum* subgroup has four cingular plates. The *Minutum* subgroup, on the other hand, does possess a transitional plate and three cingular plates.

In the *Americanum* and *Monovelum* subgroups, the sulcal fin is relatively reduced and does not extend beyond the posterior sulcal plate. In the *Minutum* subgroup, the sulcal fin is relatively large and extends beyond the posterior sulcal plate (Mertens et al. 2012a; Ribeiro et al. 2010; Yamaguchi et al. 2011). Other sulcal plates also show variation in shape between the groups. The anterior sulcal plate (Sa) shows more anterior–posterior elongation in the *Minutum* subgroup (Mertens et al. 2012a; Ribeiro et al. 2010; Yamaguchi et al. 2011), whereas its sides become more equilateral in the *Americanum* subgroup (Abé 1981; Lewis and Dodge 1987; Kawami et al. 2009; Kawami and Matsuoka 2009; this study). In the *Monovelum* subgroup, the Sa plate has an intermediate shape between these two groups (Abé 1936). This obviously affects the shape of the plates that contact this plate, particularly the right sulcal plate (Sd) and the left sulcal plate (Ss) which show similar elongation.

In the *Americanum* subgroup, the edges forming the apical collar surrounding the pore plate are low, and the shape of the pore plate can be elongated (*P. fukuyoi*, *P. americanum*, *P. fusiforme* and *P. parthenopes*) or square (*P. tricingulatum*). *Protoperidinium monovelum* of the *Monovelum* subgroup has a similar elongated pore plate with a low apical collar. Species of the *Minutum* group have elongated pore plates with high edges forming the apical collar. Within this study, we could not unfortunately observe details of the apical pores.

The texture of the theca is also group-specific. Plates of species from the *Americanum* subgroup are smooth. Plates of the *Monovelum* subgroup are granulate (K.N.M., pers. observ.). Plates of *A. minutum* and *A. saanichi* from the *Minutum* subgroup are microreticulate.

We suspect that the overlap pattern of plates in the *Americanum* subgroup are also characteristic, and may differentiate it from the *Minutum* subgroup, but unfortunately, we were unable to observe the overlap pattern in species of the *Americanum* subgroup.

Other characteristics, such as the number of anterior intercalary plates or the number of sulcal plates, are not useful for differentiating the *Americanum* subgroup from the other subgroups, as these vary too much within the *Americanum* subgroup. Other plates are constant in number: precingular, apical, postcingular and antapical plates are constant within all species of the *Monovela* group.

Comparative morphology of cysts within the Monovela group

Cysts have been documented for all species except *P. monovelum* of the *Monovelum* subgroup and *P. fusiforme* of the *Americanum* subgroup (Table 2). The archeopyle type characterizes the subgroups. Cysts within the *Americanum* subgroup have archeopyles corresponding to a combination of three apical plates, with some being saphopylic (*I. minutum* and cysts of *P. americanum*, *P. parthenopes*, and *P. fukuyoi*) and one theropylic (cyst of

P. tricingulatum). The *Minutum* subgroup on the other hand can be characterized by cysts with theropylic archeopyles corresponding to the 2a plate. It is interesting to speculate about this difference in archeopyle between both subgroups – could it be related to the noted differences in thecae such as in the apical collar, or unobserved details of the apical pore and/or overlap pattern?

Process types and indeed the presence or absence of processes do not characterize the subgroups, but are important characters at species level. Within the *Americanum* subgroup, some cysts bear processes that are acuminate or minutely expanded distally (*I. minutum* and cysts of *P. tricingulatum* and *P. fukuyoi*) and some do not have processes (cysts of *P. americanum* and *P. parthenopes*), whereas all species within the *Minutum* subgroup have processes that are minutely expanded distally. The central body texture does not seem to be subgroup-specific, as most documented wall textures are smooth. The loosely appressed outer wall layer characteristic of cysts of *P. americanum* and *P. parthenopes* is not found in any other species of the *Monovela* group.

Distribution of cysts of *P. fukuyoi*

The cyst stage is here confirmed through cyst–theca experiments from coastal British Columbia, Canada, and San Pedro Harbor, California, and we have found similar cysts over a long stretch of the northeastern Pacific (Fig. S1 and Table S1). Recent sediment trap studies from the Strait of Georgia (Pospelova et al. 2010), Saanich Inlet (Price and Pospelova 2011) and the Santa Barbara Basin (Bringué et al. 2013) show that the cyst of *P. fukuyoi* occurs locally with higher cyst fluxes in the summer and early fall months at temperatures of ~14–18 °C, salinities of 22–34 psu, and relaxed conditions after a period of active upwelling. This suggests that *P. fukuyoi* is associated with higher SST, and possibly elevated surface primary productivity.

It is likely that the species abundance, like most heterotrophic dinoflagellates, is also determined by its prey availability, likely diatoms, ciliates, dinoflagellates and other protists (e.g. Bockstahler and Coats 1993; Hansen and Calado 1999; Jacobson and Anderson 1992, 1996), which could be indirectly regulated by macronutrient availability. A similar relationship has been proposed for the large heterotrophic cyst species *Selenopemphix undulata* (Verleye et al. 2011) and *A. saanichi* (Mertens et al. 2012a). The known coastal and estuarine distribution of the cysts suggests that *P. fukuyoi* is a neritic species, and its persistent occurrences in our samples from the eastern Pacific Ocean imply a yet wider total range within the Pacific.

CONCLUSIONS

- The cyst–theca relationship in a dinoflagellate species, *P. fukuyoi* n. sp., is described through incubation experiments of cysts from sediments underlying estuarine waters off southern Vancouver Island, British Columbia, Canada and San Pedro Harbor, California, USA.
- The cyst of *P. fukuyoi* is highly distinctive, being round, brown, and spiny with acuminate processes typically arranged in linear clusters. The archeopyle is apical and saphopylic and of the *Islandinium* type.
- *Protoperidinium fukuyoi* is assigned to the *Monovela* group of Abé (1936) based on its thecal morphology.
- Molecular phylogenetics (SSU and LSU rDNA) show that *P. fukuyoi* belongs to the *Americanum* subgroup and that it is most closely related to *P. fusiforme*.
- Molecular phylogenetics (SSU and LSU rDNA) from cells of *A. minutum* collected off Japan show that these specimens are close to other *A. minutum* strains and to *A. saanichi* (*Minutum* subgroup).
- We show that the *Americanum* subgroup is characterized by species with smooth thecal plates, an apical pore plate with low apical collar, three or four cingular plates, and cysts with an archeopyle primarily comprising three apical plates. These characteristics differentiate this subgroup from the *Minutum* and *Monovelum* subgroups of the *Monovela* group.
- The cyst of *P. fukuyoi* is widely distributed along the northeastern Pacific margin where, under optimal conditions, SSTs are between ~14 and 18 °C, SSSs are between 22 and 34 psu, and surface primary productivity is possibly elevated.
- Specimens of *I. minutum* from northern Canada failed to incubate. However, molecular phylogenetic (SSU rDNA) show that this species, too, is related to the *Americanum* subgroup as it clusters within the same clade.

ACKNOWLEDGEMENTS

K.N.M. is a postdoctoral fellow of FWO Belgium and this research was partly conducted at Nagasaki University and supported by a Kakenhi grant 22-00805. This research was also partly supported by NSERC Discovery (224236) and Ship Time grants to V.P., an NSERC Discovery Grant to M.J.H., as well as a Marie Curie Career Integration Grant awarded to A.J.P. Carrie Wolfe, Adam Willingham, and Dennis Dunn from the Southern California Marine Institute, are thanked for help with sampling in San Pedro Harbor. Captain Brown and the crew of the marine sciences vessel John Strickland provided valuable assistance during the CM3 sediment core sampling cruise. Andrea Price kindly provided a sample from Brentwood Bay. The VENUS (Victoria Experimental Network Under the Sea) team is thanked for their assistance in collecting of Saanich Inlet and Strait of Georgia surface sediments. Surface sediment samples from the coastal northeastern Pacific were provided by the Scripps Institution of Oceanography (SIO), Oregon State University (OSU), Woods Hole Oceanographic Institution and the U.S. Geological Survey. We are grateful to Robbie Bennett and Bob Murphy (Geological Survey of Canada – Atlantic), and Mark Furze (Grant MacEwan University), as well as the crew of the Canadian Coastguard Vessel Amundsen, for help with sampling in Arctic Canada. V.P. is grateful to Brent Gowen (Electron Microscopy Laboratory, Biology Department, University of

Victoria) for assistance with the SEM work. Associate editor Bob Anderson and two anonymous reviewers offered comments that significantly improved the manuscript.

LITERATURE CITED

Abé, T. H. 1927. Report of the biological survey of Mutsu Bay. 3. Notes on the protozoan fauna of Mutsu Bay. I. Peridiniales. *Sci. Rep. Tohoku Imp. Uni., Biology*, 2:383–438.

Abé, T. H. 1936. Report of the biological survey of Mutsu Bay. 29. Notes on the protozoan fauna of Mutsu Bay. II. Genus *Peridinium*; subgenus *Archaeperidinium*. *Sci. Rep. Tohoku Imp. Univ., Fourth Ser., Biology*, 10:639–686.

Abé, T. H. 1981. Studies on the Family Peridiniidae. An Unfinished Monograph of the Armoured Dinoflagellata. Publications of the Seto Marine Biological Laboratory, Special Publication Series Vol. VI. Academia Scientific Book Inc., Tokyo, Japan. p. 1–413.

Balech, E. 1974. El genero *"Protoperidinium"* Bergh, 1881 *("Peridinium"* Ehrenberg, 1831, partim). *Museo Argentino de ciencias naturales "Bernardino Rivadavia" e Instituto nacional de investigación de las ciencias naturales. Revista, Hidrobiología*, 4:1–79.

Balech, E. 1988. Los dinoflagellados del Atlántico Sudoccidental. *Pub. Esp. Inst. Español Oceanografía*, 1:1–310.

Bergh, R. S. 1881. Der Organismus der Cilioflagellaten. Eine phylogenetische Studie. *Morphologisches Jahrbuch* 7:177–288, pls 12–16.

Bockstahler, K. R. & Coats, D. W. 1993. Spatial and temporal aspects of mixotrophy in Chesapeake Bay dinoflagellates. *J. Eukaryot. Microbiol.*, 40:49–60.

Bolch, C. J. S. 1997. The use of polytungstate for the separation and concentration of living dinoflagellate cysts from marine sediments. *Phycologia*, 37:472–478.

Bolch, C. J. S. 2001. PCR protocols for genetic identification of dinoflagellates directly from single cysts and plankton cells. *Phycologia*, 40:162–167.

Bringué, M., Pospelova, V. & Pak, D. 2013. Seasonal production of organic-walled dinoflagellate cysts in an upwelling system: a sediment trap study from the Santa Barbara Basin, California, *Mar. Micropaleontology*, 100:34–64.

Bütschli, O. 1885. Erster Band. Protozoa. 3. Unterabtheilung (Ordnung) Dinoflagellata. *In*: Bronn's, H.G. (ed.), Dr. H. G. Bronn's Klassen und Ordnungen des Thier-Reichs, wissenschaftlich dargestellt in Wort und Bild. C.F. Winter'sche Verlagshandlung, Leipzig und Heidelberg. p. 906–1029.

Chomérat, N. & Couté, A. 2008. *Protoperidinium bolmonense* sp. nov. (Peridiniales, Dinophyceae), a small dinoflagellate from a brackish hypereutrophic lagoon (South of France). *Phycologia*, 47:392–403.

Comeau, A. M., Philippe, B., Thaler, M., Gosselin, M., Poulin, M. & Lovejoy, C. 2013. Protists in arctic drift and land-fast sea ice. *J. Phycol.*, 49:229–240.

Fensome, R. A., Taylor, F. J. R., Norris, G., Sarjeant, W. A. S., Wharton, D. I. & Williams, G. L. 1993. A classification of living and fossil dinoflagellates. *Micropaleontology, Spec. Publ.*, 7:1–351.

Figueroa, R. I., Vázquez, J. A., Massanet, A., Murado, M. A. & Bravo, I. 2011. Interactive effects of salinity and temperature on planozygote and cyst formation in *Alexandrium minutum* (Dinophyceae) in culture. *J. Phycol.*, 47:13–24.

Gómez, F. 2005. A list of free-living dinoflagellate species in the world's oceans. *Acta Bot. Croat.*, 64:129–212.

Haeckel, E., 1894, Systematische Phylogenie. Entwurf eines natürlichen Systems der Organismen auf Grund ihrer Stammesgeschichte. 1. Theil: Systematische Phylogenie der Protisten und Pflanzen: p. I–XV + 1–400, Georg Reimer (Berlin).

Hansen, P. J. & Calado, A. J. 1999. Phagotrophic mechanisms and prey selection in free living dinoflagellates. *J. Eukaryot. Microbiol.*, 46:382–389.

Harland, R., Reid, P. C., Dobell, P. & Norris, G. 1980. Recent and sub-recent dinoflagellate cysts from the Beaufort Sea, Canadian Arctic. *Grana*, 19:211–225.

Head, M. J. 2003. *Echinidinium zonneveldiae* sp. nov., a dinoflagellate cyst from the Late Pleistocene of the Baltic Sea, northern Europe. *J. Micropalaeontol.*, 21:169–173 [Imprinted 2002].

Head, M. J., Harland, R. & Matthiessen, J. 2001. Cold marine indicators of the late Quaternary: the new dinoflagellate cyst genus *Islandinium* and related morphotypes. *J. Quaternary Sci.*, 16:621–636.

Huelsenbeck, J. P. & Ronquist, F. 2001. MRBAYES: Bayesian inference of phylogenetic trees. *Bioinformatics*, 17:754–755.

Jacobson, D. M. & Anderson, D. M. 1992. Ultrastructure of the feeding apparatus and myonemal system of the heterotrophic dinoflagellate *Protoperidinium spinulosum*. *J. Phycol.*, 28:69–82.

Jacobson, D. M. & Anderson, D. M. 1996. Widespread phagocytosis of ciliates and other protists by marine mixotrophic and heterotrophic thecate dinoflagellates. *J. Phycol.*, 32:279–285.

Kawami, H. & Matsuoka, K. 2009. A new cyst–theca relationship of *Protoperidinium parthenopes* Zingone and Montresor (Peridiniales, Dinophyceae). *Palynology*, 33:11–18.

Kawami, H., Iwataki, M. & Matsuoka, K. 2006. A new diplopsalid species *Oblea acanthocysta* sp. nov. (Peridiniales, Dinophyceae). *Plankton Benthos Res.*, 1:183–90.

Kawami, H., Van Wezel, R., Koeman, R. P. & Matsuoka, K. 2009. *Protoperidinium tricingulatum* sp. nov. (Dinophyceae), a new motile form of a round, brown, and spiny dinoflagellate cyst. *Phycol. Res.*, 57:259–267.

Krepakevich, A. & Pospelova, V. 2010. Tracing the influence of sewage discharge on coastal bays of Southern Vancouver Island (BC, Canada) using sedimentary records of phytoplankton. *Cont. Shelf Res.*, 30:1924–1940.

Lewis, J. & Dodge, J. D. 1987. The cyst–theca relationship of *Protoperidinium americanum* (Gran & Braarud) Balech. *J. Micropaleontol.*, 6:113–121.

Limoges, A., Kielt, J.-F., Radi, T., Ruíz-Fernandez, A. C. & de Vernal, A. 2010. Dinoflagellate cyst distribution in surface sediments along the south-western Mexican coast (14.76 °N to 24.75 °N). *Mar. Micropaleontol.*, 76:104–123.

Maddison, D. R. & Maddison, W. P. 2000. MacClade 4: Analysis of Phylogeny and Character Evolution Version 4.0. Sinauer Associates, Sunderland, MA. 398 p.

Matsuoka, K. 1988. Cyst–theca relationships in the diplopsalid group (Peridiniales, Dinophyceae). *Rev. Palaeobot. Palynol.*, 56:95–122.

Matsuoka, K. & Kawami, H. in press. Phylogenetic subdivision of the genus *Protoperidinium* (Peridiniales, Dinophyceae) with emphasis on the *Monovela* Group. *In*: Lewis, J. M., Marret, F. & Bradley, L. (ed.), Biological and Geological Perspectives of Dinoflagellates. The Micropalaeontological Society, Special Publications. Geological Society, London. p. 267–276.

Matsuoka, K. & Head, M. J. in press. Clarifying cyst–motile stage relationships in dinoflagellates. *In*: Lewis, J. M., Marret, F. & Bradley, L. (ed.), Biological and Geological Perspectives of Dinoflagellates. The Micropalaeontological Society, Special Publications. Geological Society, London. p. 317–342.

Matsuoka, K., Noriko, N., Kawami, H. & Iwataki, M. 2006. New method for establishing the cyst–motile form relationship in dinoflagellates. *Fossils* 80:33–40. [In Japanese]

Matsuoka, K., Kawami, H., Nagai, S., Iwataki, M. & Takayama, H. 2009. Re-examination of cyst–motile relationships of *Polykrikos kofoidii* Chatton and *Polykrikos schwartzii* Bütschli (Gymnodiniales, Dinophyceae). *Rev. Palaeobot. Palynol.*, 154:79–90.

Mertens, K. N., Yamaguchi, A., Kawami, H., Ribeiro, S., Leander, B. S., Price, A. M., Pospelova, V., Ellegaard, M. & Matsuoka, K. 2012a. *Archaeperidinium saanichi* sp. nov.: a new species based on morphological variation of cyst and theca within the *Archaeperidinium minutum* Jörgensen 1912 species complex. *Mar. Micropaleontol.*, 96–97:48–62.

Mertens, K. N., Bradley, L. R., Takano, Y., Mudie, P. J., Marret, F., Aksu, A. E., Hiscott, R. N., Verleye, T. J., Mousing, E. A., Smyrnova, L. L., Bagheri, S., Mansor, M., Pospelova, V. & Matsuoka, K. 2012b. Quantitative estimation of Holocene surface salinity variation in the Black Sea using dinoflagellate cyst process length. *Quat. Sci. Rev.*, 39:45–59.

Mertens, K. N., Bringué, M., Van Nieuwenhove, N., Takano, Y., Pospelova, V., Rochon, A., de Vernal, A., Radi, T., Dale, B., Patterson, R. T., Weckström, K., Andrén, E., Louwye, S. & Matsuoka, K. 2012c. Process length variation of the cyst of the dinoflagellate *Protoceratium reticulatum* in the North Pacific and Baltic–Skagerrak region: calibration as annual density proxy and first evidence of pseudo-cryptic speciation. *J. Quaternary Sci.*, 27:734–744.

Nakayama, T., Watanabe, S., Mitsui, K., Uchida, H. & Inouye, I. 1996. The phylogenetic relationship between the Chlamydomonadales and Chlorococcales inferred from 18S rDNA sequence data. *Phycol. Res.*, 44:47–55.

Pascher, A. 1914. Über Flagellaten und Algen. *Berichte der Deutschen Botanischen Gesellschaft*, 32:136–160.

Posada, D. 2008. jModelTest: phylogenetic model averaging. *MBE*, 25:1253–1256.

Pospelova, V. & Head, M. J. 2002. *Islandinium brevispinosum* sp. nov. (Dinoflagellata), a new organic-walled dinoflagellate cyst from modern estuarine sediments of New England (USA). *J. Phycol.*, 38:593–601.

Pospelova, V., Chmura, G. L. & Walker, H. A. 2004. Environmental factors influencing spatial distribution of dinoflagellate cyst assemblages in shallow lagoons of southern New England (USA). *Rev. Palaeobot. Palynol.*, 128:7–34.

Pospelova, V., Pedersen, T. F. & de Vernal, A. 2006. Dinoflagellate cysts as indicators of climatic and oceanographic changes during the past 40 kyr in the Santa Barbara Basin, southern California. *Paleoceanography*, 21, PA2010. doi:10.1029/2005PA001251

Pospelova, V., de Vernal, A. & Pedersen, T. F. 2008. Distribution of dinoflagellate cysts in surface sediments from the northeastern Pacific Ocean (43–25° N) in relation to sea-surface temperature, salinity, productivity and coastal upwelling. *Mar. Micropaleontol.*, 68:21–48.

Pospelova, V., Esenkulova, S., Johannessen, S. C., O'Brien, M. C. & Macdonald, R. W. 2010. Organic-walled dinoflagellate cyst production, composition and flux from 1996 to 1998 in the central Strait of Georgia (BC, Canada): a sediment trap study. *Mar. Micropaleontol.*, 75:17–37.

Price, A. M. & Pospelova, V. 2011. High-resolution sediment trap study of organic-walled dinoflagellate cyst production and biogenic silica flux in Saanich Inlet (BC, Canada). *Mar. Micropaleontol.*, 80:18–43.

Price, A. M., Mertens, K. N., Pospelova, V., Pedersen, T. F. & Ganeshram, R. S. 2013. Late Quaternary climatic and oceanographic changes in the Northeast Pacific as recorded by dinoflagellate cysts from Guaymas Basin, Gulf of California (Mexico). *Paleoceanography*, 28: 1–13.

Radi, T., Pospelova, V., de Vernal, A. & Barrie, J. V. 2007. Dinoflagellate cysts as indicators of water quality and productivity in British Columbia estuarine environments. *Mar. Micropaleontol.*, 62:269–297.

Radi, T., Bonnet, S., Cormier, M.-A., de Vernal, A., Durantou, L., Faubert, E., Head, M. J., Henry, M., Pospelova, V., Rochon, A. & Van Nieuwenhove, N. 2013. Operational taxonomy for round, brown, spiny dinocysts from high latitudes of the Northern Hemisphere. *Mar. Micropaleontol.*, 98:41–57.

Ribeiro, S., Lundholm, N., Amorim, A. & Ellegaard, M. 2010. *Protoperidinium minutum* (Dinophyceae) from Portugal: cyst–theca relationship and phylogenetic position on the basis of single-cell SSU and LSU rDNA sequencing. *Phycologia*, 49:48–63.

Rochon, A. Potvin, E. 2006. Cyst–theca relationships of *Islandinium minutum*. *In*: Poulsen, N. (ed.), 2006 International Workshop on Dinoflagellates and Their Cysts: Their Ecology and Databases for Paleoenvironmental Reconstructions, p. 29–30. GEUS report 2008/78, Geological survey of Denmark and Greenland, Copenhagen.

Siano, R. & Montresor, M. 2005. Morphology, ultrastructure and feeding behaviour of *Protoperidinium vorax* sp. nov. (Dinophyceae, Peridiniales). *Eur. J. Phycol.*, 40:221–32.

von Stosch, H. A. 1973. Observations on vegetative reproduction and sexual life cycles of two freshwater dinoflagellates, *Gymnodinium pseudopalustre* Schiller and *Woloszynskia apiculata* sp. nov. *Br. Phycol. J.*, 8:105–134.

Takano, Y. & Horiguchi, T. 2006. Acquiring scanning electron microscopical, light microscopical and multiple gene sequence data from a single dinoflagellate cell. *J. Phycol.*, 42(1):251–256.

Verleye, T. J., Pospelova, V., Mertens, K. N. & Louwye, S. 2011. The geographical distribution and (palaeo)ecology of *Selenopemphix undulata* sp. nov., a new late Quaternary dinoflagellate cyst from the Pacific Ocean. *Mar. Micropaleontol.*, 78:65–83.

Wall, D. & Dale, B. 1968. Modern dinoflagellate cysts and evolution of the Peridiniales. *Micropaleontology*, 14:265–304.

Watanabe, M. M., Kawachi, M., Hiroki, M. & Kasai, F. 2000. NIES-Collection. List of Strains. Microalgae and Protozoa, 6th ed. National Institute of Environmental Studies, Tsukuba, Japan. 159 p.

Yamaguchi, A., Hoppenrath, M., Pospelova, V., Horiguchi, T. & Leander, B. S. 2011. Molecular phylogeny of the marine sand-dwelling dinoflagellate *Herdmania litoralis* and an emended description of the closely related planktonic genus *Archaeperidinium* Jörgensen. *Eur. J. Phycol.*, 46:98–112.

Zingone, A. & Montresor, M. 1988. *Protoperidinium parthenopes* sp. nov. (Dinophyceae), an intriguing dinoflagellate from the Gulf of Naples. *Cryptogamie: Algol*, 9:117–125.

Zonneveld, K. A. F. 1997. New species of organic-walled dinoflagellate cysts from modern sediments of the Arabian Sea (Indian Ocean). *Rev. Palaeobot. Palynol.*, 97:319–337.

Zonneveld, K. A. F. & Dale, B. 1994. The cyst–motile stage relationships of *Protoperidinium monospinum* (Paulsen) Zonneveld et Dale comb. nov. and *Gonyaulax verior* (Dinophyta, Dinophyceae) from the Oslo Fjord (Norway). *Phycologia*, 33:359–368.

Zonneveld, K. A. F., Marret, F., Versteegh, G., Bogus, K., Bonnet, S., Bouimetarhan, I., Chen, L., Crouch, E., de Vernal, A., Elshanawany, R., Edwards, L., Esper, O., Forke, S., Grøsfjeld, K., Henry, M., Holzwarth, U., Kielt, J.-F., Kim, S.-Y., Ladouceur, S., Ledu, D., Limoges, A., Londeix, L., Lu, S.-H., Mahmoud, M. S., Marino, G., Matsouka [sic], K., Matthiessen, J., Mildenhal [sic], D. C., Mudie, P., Neil, H. L., Pospelova, V.,

Qi, Q., Radi, T., Richerol, T., Rochon, A., Sangiorgi, F., Solignac, S., Turon, J.-L., Verleye, T., Wang, Y., Wang, Z. & Young, M. 2013. Atlas of dinoflagellate cyst distribution based on 2405 datapoints. *Rev. Palaeobot. Palynol.*, doi:10.1016/j.revpalbo.2012.08.003, 1-441.

Zwickl, D. J. 2006. Genetic algorithm approaches for the phylogenetic analysis of large biological sequence datasets under the maximum likelihood criterion. Ph.D. dissertation. The University of Texas, Austin.

SUPPORTING INFORMATION

Additional Supporting Information may be found in the online version of this article:

Figure S1. Sampling locations for incubation experiments and single-cell PCR (Table 1) and palynologically prepared samples from surface sediments and sediment traps (Table S1). Detailed insets show samples used for incubation experiments of *Protoperidinium fukuyoi* sp. nov. from San Pedro Harbor (California) and around Vancouver Island (British Columbia). Specimens of *Islandinium minutum* used for single-cyst PCR analyses were collected from Barrow Strait, Nunavut, Canada.

Table S1. Details of sampling locations of palynologically prepared samples from surface sediments and sediment traps.

Supporting information

Figure S1. Sampling locations for incubation experiments and single-cell PCR (Table 1) and palynologically prepared samples from surface sediments and sediment traps (Table S1). Detailed insets show samples used for incubation experiments of *Protoperidinium fukuyoi* sp. nov. from San Pedro Harbor (California) and around Vancouver Island (British Columbia). Specimens of *Islandinium minutum* used for single-cyst PCR analyses were collected from Barrow Strait, Nunavut, Canada.

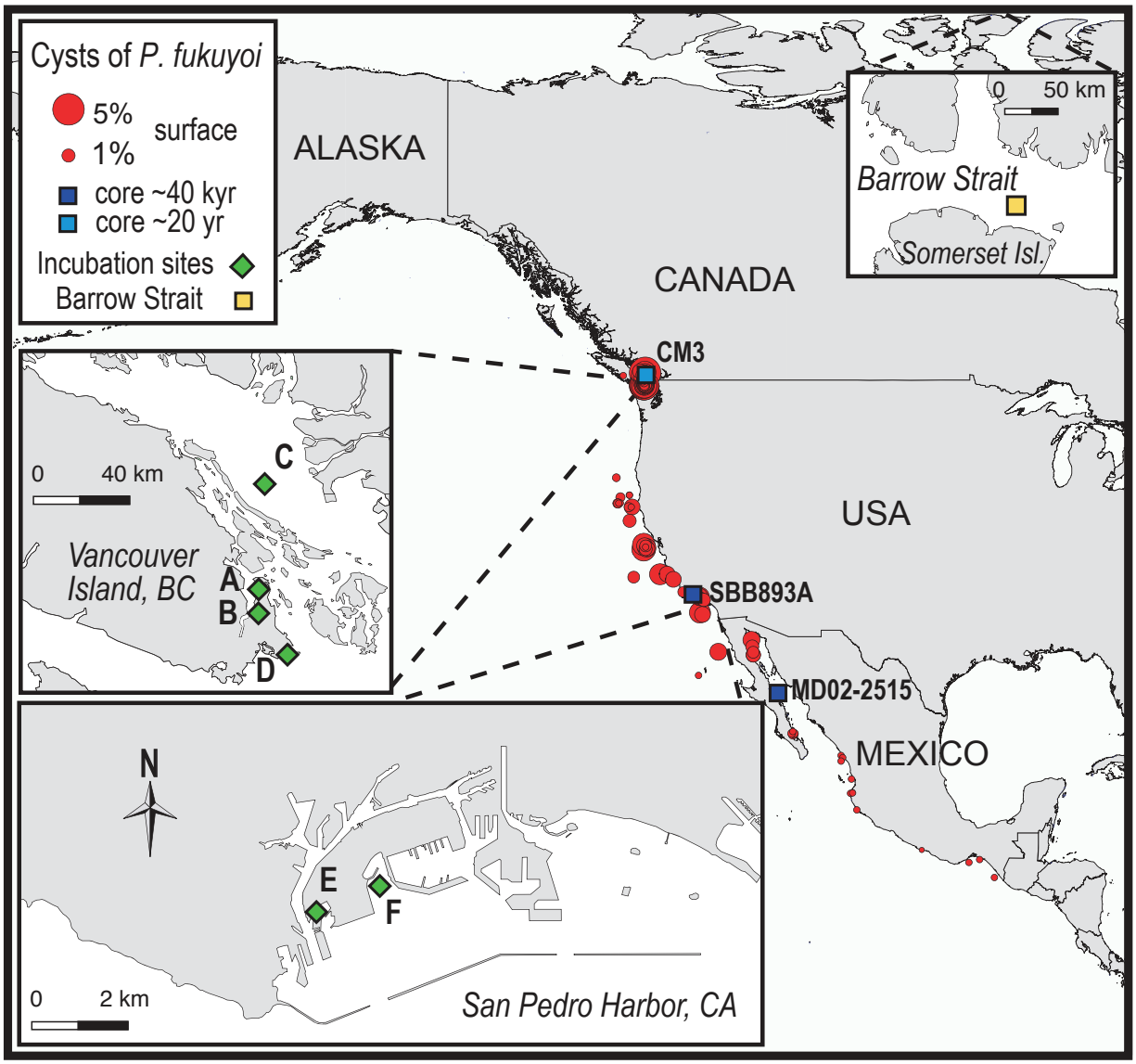

Table S1: details of sampling locations of palynologically prepared samples from surface sediments and sediment traps.

Sampled by	Station	Latitude (°N)	Longitude (°W)	Water depth (m)	Lab	ID	Sampling device	% cysts of *P. fukuyoi*	Ref
Tul92	10	49.260	-123.295	66	UQ	1871-3	BG	4.8	(1)
Tul92	34	49.200	-123.428	289	UQ	1871-6	BG	0.6	(1)
Tul92	36	49.211	-123.373	243	UQ	1861-4	BG	1.9	(1)
Tul92	50	49.249	-123.443	256	UQ	1872-2	BG	0.6	(1)
Tul92	51	49.235	-123.444	302	UQ	1872-3	BG	1.5	(1)
Tul92	129	49.284	-123.465	178	UQ	1873-4	BG	0.5	(1)
Tul92	135	49.287	-123.165	13	UQ	1873-5	BG	1.0	(1)
Tul92	140	49.318	-123.285	129	UQ	1873-6	BG	1.6	(1)
Tul92	143	49.322	-123.348	184	UQ	1874-1	BG	1.3	(1)
Tul92	159	49.290	-123.311	107	UQ	1874-2	BG	2.7	(1)
Tul92	169	49.011	-123.472	228	UQ	1874-5	BG	2.0	(1)
Vec03	30	49.305	-123.189	25	UQ	1912-6	BG	0.8	(1)
Vec03	47	49.371	-123.746	192	UQ	1913-4	BG	1.3	(1)
Vec03	66	49.139	-123.558	345	UQ	1916-1	BG	2.5	(1)
Vec03	68	49.119	-123.572	268	UQ	1916-2	BG	0.9	(1)
Vec03	73	48.912	-123.325	97	UQ	1916-4	BG	0.4	(1)
OSU	3	40.751	-125.404	2934	UQ	1917-2	B	0.6	(2)
OSU	4	39.155	-124.614	3330	UQ	1917-3	B	1.1	(2)
OSU	5	42.093	-125.755	2782	UQ	1917-4	B	0.4	(2)
OSU	10	40.360	-125.420	1584	UQ	1918-3	G	0.3	(2)
OSU	11	40.346	-125.660	1869	UQ	1918-4	G	0.5	(2)
OSU	12	40.352	-125.550	1668	UQ	1918-5	G	0.3	(2)

OSU	13	40.335	-125.605	1879	UQ	1918-6	G	0.5	(2)
SIO	15	40.903	-124.648	637	UQ	1919-4	B	0.3	(2)
SIO	17	40.093	-124.477	720	UQ	1920-1	B	0.3	(2)
SIO	18	40.100	-124.408	600	UQ	1920-2	B	1.5	(2)
SIO	19	40.083	-124.687	940	UQ	1920-3	B	0.6	(2)
SIO	20	40.902	-124.630	620	UQ	1920-4	B	0.3	(2)
SIO	21	35.503	-121.397	630	UQ	1920-5	B	1.4	(2)
SIO	22	35.458	-121.517	940	UQ	1920-6	B	3.3	(2)
SIO	23	35.500	-122.010	1545	UQ	1921-1	B	2.4	(2)
OSU	24	29.983	-114.017	433	UV	2004-189	G	1.2	(2)
OSU	28	29.983	-114.000	448	UV	2004-193	B	1.3	(2)
WHOI	30	30.163	-114.018	335	UV	2004-195	G	0.9	(2)
WHOI	31	31.009	-114.165	210	UV	2004-196	G	1.7	(2)
WHOI	32	30.559	-114.100	154	UV	2004-197	G	1.0	(2)
USGSMP	33	37.216	-123.409	3120	UQ	1998-1	G	3.1	(2)
USGSMP	34	37.224	-123.244	1605	UQ	1998-4	G	1.1	(2)
USGSMP	35	37.527	-123.408	2495	UQ	1998-6	G	2.6	(2)
USGSMP	36	37.449	-123.333	1720	UQ	1999-1	G	1.5	(2)
USGSMP	37	37.433	-123.243	1378	UQ	1999-2	G	0.8	(2)
USGSMP	38	37.310	-123.154	1050	UQ	1999-3	G	1.9	(2)
USGSMP	39	37.311	-123.154	1050	UQ	1999-6	G	1.2	(2)
USGSMP	40	37.242	-123.074	685	UQ	2000-1	G	1.3	(2)
USGSMP	41	37.356	-123.248	1260	UQ	2000-2	G	0.3	(2)
USGSMP	42	33.979	-118.575	60	UQ	1997-1	B	1.8	(2)
USGSMP	43	33.971	-118.652	182	UQ	1997-2	B	1.6	(2)
USGSMP	44	33.839	-118.551	108	UQ	1997-4	B	1.0	(2)
USGSMP	45	33.887	-118.478	53	UQ	1997-5	B	0.9	(2)
SIO	47	32.885	-118.592	349	UQ	2100-1	GR	2.5	(2)

SIO	48	32.755	-118.370	353	UV	2100-2	GR	1.5	(2)
SIO	50	28.583	-118.700	3470	UV	2005-281	G	0.3	(2)
SIO	51	35.300	-124.267	4170	UV	2005-282	G	0.9	(2)
SIO	55	30.193	-117.013	2920	UV	2005-287	G	1.6	(2)
UVic	1	48.387	-123.470	40	UV	2008-1	B	0.9	(3)
UVic	6	48.442	-123.444	11	UV	2008-6	G	0.5	(3)
UVic	7	48.431	-123.443	16	UV	2008-7	G	0.6	(3)
UVic	8	48.413	-123.439	52	UV	2008-8	G	0.6	(3)
UVic	10	48.395	-123.404	62	UV	2008-10	B	0.9	(3)
UVic	11	48.401	-123.399	70	UV	2008-11	B	0.8	(3)
UVic	14	48.399	-123.421	57	UV	2008-14	B	2.0	(3)
UVic	16	48.405	-123.390	65	UV	2008-16	B	4.2	(3)
UVic	17	48.410	-123.424	50	UV	2008-17	B	3.6	(3)
UVic	18	48.410	-123.411	55	UV	2008-18	B	4.1	(3)
UVic	19	48.416	-123.405	15	UV	2008-19	B	0.6	(3)
UVic	20	48.402	-123.359	17	UV	2008-20	B	2.2	(3)
UVic	24	48.398	-123.344	40	UV	2008-24	B	4.2	(3)
UVic	26	48.395	-123.348	64	UV	2008-26	B	3.2	(3)
UVic	28	48.389	-123.347	100	UV	2008-28	B	0.5	(3)
UVic	29	48.418	-123.392	11	UV	2008-29	B	1.6	(3)
UVic	33	48.455	-123.292	8	UV	2008-33	G	1.9	(3)
UVic	34	48.450	-123.287	9	UV	2008-34	G	2.0	(3)
UVic	35	48.440	-123.276	20	UV	2008-35	G	1.4	(3)
UVic	37	48.468	-123.284	12	UV	2008-37	G	1.7	(3)
UVic	39	48.478	-123.280	36	UV	2008-39	B	1.0	(3)
UVic	40	48.475	-123.296	12	UV	2008-40	G	1.6	(3)
UVic	44	48.507	-123.341	10	UV	2008-44	B	1.4	(3)
UVic	50	48.629	-123.385	29	UV	2008-249	B	0.6	(3)

UVic	52	48.634	-123.384	19	UV	2008-250	B	1.5	(3)
UVic	58	48.671	-123.403	8	UV	2008-255	B	0.3	(3)
UVic	60	48.596	-123.380	9	UV	2008-259	B	2.4	(3)
VENUS	SI	48.651	-123.486	96	UV	2009-644	B	0.3	(4)
SPR	10	34.222	-120.028	571	UV	2010-57	B	2.1	(5)
UVic	CM3	49.109	-123.496	355	UV	2008-215	G	0.3	(6)
Paleo IX	2	24.543	-110.610	334	UQ	2098-1	B	0.5	(7)
Paleo IX	3	24.551	-110.490	282	UQ	2098-2	B	0.4	(7)
Paleo IX	5	24.621	-110.490	34	UQ	2098-3	B	0.4	(7)
Paleo IX	7	24.620	-110.720	29.5	UQ	2098-4	B	0.4	(7)
Paleo IX	12	24.750	-110.623	324	UQ	2098-6	B	0.3	(7)
TEHUA V	13	23.109	-106.476	61.4	UQ	2407-01	B	0.3	(7)
TEHUA V	14	22.960	-106.336	60.7	UQ	2407-02	B	0.3	(7)
TEHUA V	16	22.720	-106.479	366	UQ	2407-04	B	0.3	(7)
TEHUA V	20	21.500	-105.582	60	UQ	2408-02	B	0.3	(7)
TEHUA V	24	20.524	-105.664	1400	UQ	2408-06	B	0.3	(7)
TEHUA V	25	20.550	-105.490	1127	UQ	2420-01	B	0.3	(7)
TEHUA V	32	19.386	-105.125	587.6	UQ	2421-03	B	0.3	(7)
TEHUA V	57	16.648	-99.562	51.5	UQ	2427-03	B	0.2	(7)
TEHUA	61	15.797	-95.510	225	UQ	1946-1	B	0.3	(7)
TEHUA	77	15.999	-94.600	52	UQ	2068-6	B	0.3	(7)
TEHUA	94	14.764	-93.330	258	UQ	2070-5	B	0.3	(7)
OSU-CTC	3A	49.072	-125.158	118	UV	2006-293	ST	0.3	(8)
ODP	893 A	34.288	-120.037	576	UV	2003-01/49	APC	0.7 av.	(9)
MD	MD02-2515	27.484	-112.074	881	UV	2006-543/871	GPC	0.8 av.	(10)

1 = Radi et al. (2007); 2 = Pospelova et al. (2008); 3 = Krepakevich and Pospelova (2010); 4 = Price and Pospelova (2011); 5 = Bringué et al. (in press); 6 = Pospelova et al. (2010); 7 = Limoges et al. (2010); 8 = Mertens et al. (2012c); 9 =Pospelova et al. (2006); 10 = Price et al. (2013).

UQ = UQAM; UV = Uvic; BG = Box/Gravity; B = Box core; G = Gravity core; GR = Grab; ST = Sediment trap, 30 m above bottom; APC = Advanced Piston Core; GPC = Giant Piston Core